We are IntechOpen, the world's leading publisher of Open Access books Built by scientists, for scientists

6,900
Open access books available

185,000
International authors and editors

200M
Downloads

Our authors are among the

154
Countries delivered to

TOP 1%
most cited scientists

12.2%
Contributors from top 500 universities



WEB OF SCIENCE™

Selection of our books indexed in the Book Citation Index in Web of Science™ Core Collection (BKCI)

Interested in publishing with us?
Contact book.department@intechopen.com

Numbers displayed above are based on latest data collected.
For more information visit www.intechopen.com



Chapter

AI Modeling to Combat COVID-19 Using CT Scan Imaging Algorithms and Simulations: A Study

Naser Zaeri

Abstract

The coronavirus disease 2019 (COVID-19) outbreak has been designated as a worldwide pandemic by World Health Organization (WHO) and raised an international call for global health emergency. In this regard, recent advancements of technologies in the field of artificial intelligence and machine learning provide opportunities for researchers and scientists to step in this battlefield and convert the related data into a meaningful knowledge through computational-based models, for the task of containment the virus, diagnosis and providing treatment. In this study, we will provide recent developments and practical implementations of artificial intelligence modeling and machine learning algorithms proposed by researchers and practitioners during the pandemic period which suggest serious potential in compliant solutions for investigating diagnosis and decision making using computerized tomography (CT) scan imaging. We will review the modern algorithms in CT scan imaging modeling that may be used for detection, quantification, and tracking of Coronavirus and study how they can differentiate Coronavirus patients from those who do not have the disease.

Keywords: Artificial intelligence, COVID-19, CT algorithms, modeling

1. Introduction

Today, the world is facing one of its most dangerous risks, if not the most one throughout the century. It is a pandemic that is draining the whole world's resources and threatening the development of human civilization. The COVID-19 pandemic continues to have a devastating effect on the health and well-being of global population, caused by the infection of individuals by the severe acute respiratory syndrome coronavirus 2 (SARS-CoV-2) [1]. On the 30th of January 2020, the WHO declared the SARS-CoV-2 outbreak a public health emergency of international concern. On March 11th, WHO characterized COVID-19 as a pandemic. At the time of writing this manuscript (May 29, 2021), the number of infected people has surpassed 169,118,995 confirmed cases and more than 3,519,175 deaths in 223 countries [2]. The World Trade Organization has announced that the world has effectively entered a recession period. The world's economy and many countries' economies are

in danger of collapsing. Schools in many countries are closed and students around the world are forced to stay at home [3, 4].

One of the early challenges that emerged at the beginning of the pandemic is the detection of COVID-19 cases. The most important method used for detecting COVID-19 cases is polymerase chain reaction (PCR) testing, that can detect SARSCoV-2 RNA from respiratory specimens [5]. Though PCR testing is the standard, it is a time-consuming, laborious, and complicated manual process that is in short supply [6]. Accurate and rapid diagnosis of COVID-19 suspected cases plays a crucial role in timely quarantine and medical treatment. This limitation of human expert-based diagnosis has provided a strong motivation for the use of computer simulation and modeling to improve the speed and accuracy of the detection process [7, 8]. Another related issue is the manual contouring of lung lesions which tends to be a tedious and time-consuming work, and could lead to subsequent assessment discrepancies in case of inconsistent delineation. Thus, a fast auto-contouring tool for COVID-19 infection is needed in the onsite applications for quantitative disease assessment [9].

Since the early days of this catastrophic crisis, there has been an upsurge in the exploration and use of artificial intelligence (AI), computer simulation, and data modeling and analytic tools, in a multitude of areas. AI and machine learning (ML) have demonstrated great performance in various medical fields and have proven their vital role in complicated therapeutic scenes. These systems have shown high level of accuracy in different applications, such as lung disease classification, breast cancer, skin lesion classification, identifying diabetic retinopathy, and Alzheimer [10–12].

Scientists and healthcare professionals have realized the importance of AI and imaging technologies in slowing the spread of COVID-19 at preliminary stages, and containing the virus at later stages. Currently, many AI and computer modeling systems are used in disease diagnosis, examining, identifying, and treating patients. AI-based simulations have also been employed for evaluating disease progression, economic downturn and recovery, contingency planning, demand sensing, supply chain disruptions, workforce planning, as well as for management decision-making on site openings [13]. For example, AI-based simulations were critical in integrating multiple decision-making domains (e.g., COVID-19 disease progression, government interventions, people behavior, demand sensing, supply disruptions etc.) [14].

In this paper, we provide an extensive review and a deep study on how AI and ML can help the world to deliver efficient responses and combat the COVID-19 pandemic using CT scan imaging. More specifically, we will focus on the modern algorithms in CT scan imaging that may be used for detection, quantification, and tracking of Coronavirus and study how they can differentiate Coronavirus patients from those who do not have the disease. We provide recent theoretical developments, technological advancements, and practical implementations of AI algorithms and ML techniques that uses CT imaging to suggest possible solutions in investigating diagnosis, severity level, prediction, tracking, treatments and other decision making scenarios related to COVID-19. In this regard, we explore a vast number of important studies that have been performed by various academic and research communities from numerous disciplines during the period of pandemic since the early days of 2020 up to the very recent days (May 2021). Before we further proceed, we note that many of the articles cited are still preprints at the time of writing this manuscript. Given the fast-moving nature of the crisis, we endeavored to be comprehensive of coverage. We understand that the full scientific rigor for many articles should still be assessed by the scientific community through peer-reviewed evaluation and other quality control mechanisms. However, the whole story is a striking dilemma and a big challenge to the global scientific communities.

Researchers, physicians, technical-background individuals, and academics are putting all their efforts to come up with solutions and cures to this fatal disease. All of these efforts have emerged during a very short period of time, and a lot are yet to emerge in the coming few months, and possibly years.

1.1 A view of AI and ML in healthcare

AI is becoming one of the highest priorities for healthcare decision makers, governments, investors and innovators. An increasing number of governments have set out targets for AI in healthcare, in countries as diverse as the United States, China, Finland, Germany, and the UK, and many are investing heavily in AI-related research. The private sector is also playing a significant role, with venture capital funding for the top 50 firms in healthcare-related AI reaching $8.5 billion [15]. Though the US dominates the list of firms with highest venture capital funding in healthcare AI to date, and has the most related research studies and trials, China is emerging as the fastest growing country in this field. Europe, meanwhile, benefits from the vast depot of health data collected by national health systems and has significant strengths in terms of the number of research studies, established clusters of innovation and collaborations related to AI [16].

AI applications based on imaging, are already in use in specialties such as radiology, oncology, cardiology, neurology, pathology and ophthalmology. It is expected that more AI solutions would support the shift from hospital-based to home-based care, such as remote monitoring, AI-powered alerting systems, and virtual assistants [17, 18]. Also, AI is anticipated to be embedded more extensively in clinical workflows through the intensive engagement of professional bodies and providers. Moreover, AI solutions are expected to emerge in clinical practices based on evidence from clinical trials, with increasing focus on improved and scaled clinical decision-support tools [19]. Advances in AI mean that algorithms can generate layers of abstract features that enable computers to recognize complicated concepts (such as a diagnosis). This enables them to learn discriminative features automatically and approximate highly complex relationships [20, 21].

2. Convolutional neural network

Neural networks have been successfully applied to many real-world problems. The most general type of neural network is Multilayer Perceptron (MLP). While MLPs can be used to effectively classify small images, they are impractical for large images. The reason for this can be explained by the fact that the implementation of a MLP would result in a huge output vector of weights for each class (size of millions). MLPs not only are computationally expensive to train (both in terms of time and memory usage), but they also have high variance due to the large number of weights [22, 23].

Convolutional Neural Networks (CNNs) have been driving the heart of computer vision in recent years. The key concept of CNNs is to find local features from an input (usually an image) at higher layers and combine them into more multifaceted features at lower layers [24, 25]. CNNs are very good in extracting patterns in the input image, such as lines, gradients, circles, or even eyes and faces. It is this property that makes CNNs so powerful for computer vision. Unlike earlier computer vision algorithms, CNNs can operate directly on a raw image and do not need any preprocessing. In the medical field, CNNs are used to improve image quality in low-light images from a high-speed video endoscopy [26] and is also applied to recognize the nature of pulmonary nodules via CT images and the identification of pediatric pneumonia via chest X-ray images [27].

A CNN comprises several layers where each neuron of a subsequent higher layer connects to a subset of neurons in the previous lower layer. This permits the receptive field of a neuron of a higher layer to cover a greater part of images compared to that of a lower layer. The higher layer is capable to learn more abstract features of images than the lower layer by considering the spatial relationships between different receptive fields. It should be noted that CNNs significantly reduce the number of weights, and in turn reduce the variance. Like MLPs, CNNs use fully connected (FC) layers and non-linearities, but they introduce two new types of layers: convolutional and pooling layers. A convolutional layer takes a W × H × D dimensional input "I" and convolves it with a w × h × D dimensional filter (or kernel) G. The weights of the filter can be hand designed, but in the context of machine learning they are automatically tuned, just like the way weights of an FC layer are tuned. In line with convolutional layers where reducing the number of weights in neural networks reduces the variance, pooling layers directly reduce the number of neurons in neural networks. The sole purpose of a pooling layer is to downsample (also known as pool, gather, consolidate) the previous layer, by sliding a fixed window across a layer and choosing one value that effectively "represents" all of the units captured by the window. There are two common implementations of pooling. In max-pooling, the representative value just becomes the largest of all the units in the window, while in average-pooling, the representative value is the average of all the units in the window. In practice, pooling layers are stridden across the image with the stride equal to the size of the pooling layer. None of these properties actually involve any weights, unlike fully connected and convolutional layers.

3. CT diagnosis algorithms

Medical imaging is a useful supplement to reverse transcription polymerase chain reaction (RT-PCR) testing for the confirmation of COVID-19. Researchers have found that CT images of COVID-19 patients exhibit typical imaging characteristics. During the last year, studies have shown that typical chest CT patterns of COVID-19 viral pneumonia include multifocal bilateral peripheral ground-glass areas associated with subsegmental patchy consolidations, mostly subpleural, and predominantly involving lower lung lobes and posterior segments [28–32]. In more detail, chest CT images of COVID-19 patients could be evaluated using the following characteristics [33–40]:

- presence of ground-glass opacities (GGOs)
- laterality of GGO and consolidation
- presence of nodules
- presence of pleural effusion
- presence of thoracic lymphadenopathy
- degree of involvement of each lung lobe, in addition to the overall extent of lung involvement measured
- presence of underlying lung disease such as emphysema or fibrosis
- bilateral distribution

- number of lobes affected where either ground-glass or consolidative opacities are present
- interlobular septal thickening
- presence of cavitation
- bronchial wall thickening
- air bronchogram
- perilesional vessel diameter
- lymphadenopathy
- pleural pericardial effusion

GGO, which is defined as hazy increased lung attenuation with preservation of bronchial and vascular margins [41], is the most common early finding of COVID-19 on chest CT. Besides GGO, bilateral patchy shadowing is one of the most common radiologic findings on chest CT [42]. In another study containing 51 COVID-19 patients, Song et al. [43] found that disease progression can be determined by lesions with consolidation. Multiple lesions and crazy-paving pattern are also common in COVID-19 patients. The diagnosis of chest CT depending on visual diagnosis of radiologists suffers from some problems [44]. For example, chest CT contains hundreds of slices, which takes a long time to diagnose. Also, it was found that the chest CT images of some COVID-19 patients share some similar manifestations with other types of pneumonia. This could add extra challenges to inexperienced radiologists, considering that COVID-19 is a new lung disease.

During the last year, AI methods and ML techniques have played a very important role in COVID-19 diagnosis in applications utilizing the CT imaging. The aim of AI techniques and ML methods was always to extract the distinguished features of COVID-19 presented in the different types of images. In this section, we review and thoroughly discuss the major works and articles that have addressed AI and ML in COVID-19 diagnosis using CT imagery. AI and deep learning methods have shown great ability to address the aforementioned problems by detecting this disease and distinguishing it from community acquired pneumonia (CAP) and other non-pneumonic lung diseases using chest CT. We explore important studies that have been performed by various academic and research communities from numerous disciplines which focus on detecting, quantifying, and tracking of Coronavirus and study how they can differentiate Coronavirus patients from those who do not have the disease.

Li et al. [45] developed a 3D deep learning framework for the detection of COVID-19, referred to as COVID-19 detection neural network (COVNet). The proposed CNN consists of a RestNet50 as the backbone, which takes a series of CT slices as the input and generates features for the corresponding slices. In more detail, it extracts visual features from volumetric chest CT scans both in 2D local and 3D global representation. The extracted features from all slices are then combined by a max-pooling operation. CAP and other non-pneumonia CT scans were included to test the robustness of the proposed model. The final feature map is fed to a fully connected layer and softmax activation function to generate a probability score for each type (COVID-19, CAP, and non-pneumonia), and produce a classification prediction. The CT scans are performed using different manufacturers with

standard imaging protocols. Each volumetric scan contains 1094 CT slices with a varying slice-thickness from 0.5 mm to 3 mm. The reconstruction matrix is 512x512 pixels with in-plane pixel spatial resolution from 0.29x0.29 mm^2 to 0.98x0.98 mm^2. The CT scans are preprocessed and the lung region is extracted as the region of interest (ROI) using a U-net based segmentation method. Then, the image is passed to the COVNet for the predictions, as shown in **Figure 1**.

The authors have tested the system on datasets collected from six hospitals between August 2016 and February 2020. The collected datasets consisted of 4356 chest CT scans from 3322 patients. Diagnostic performance was assessed by the area under the receiver operating characteristic curve (AUC), sensitivity and specificity. The COVID-19 cases were affirmed as positive by RT-PCR and were obtained from Dec 31, 2019 to Feb 17, 2020. The most shared symptoms were fever (81%) and cough (66%). Moreover, the patients were 49±15 years old and there are slightly more male patients than female (1838 vs. 1484). CT scans with multiple reconstruction kernels at the same imaging session or acquired at multiple time points were included. The final dataset consisted of 1296 (30%) scans for COVID-19, 1735 (40%) for CAP and 1325 (30%) for non-pneumonia.

For each patient, one or multiple CT scans at several time points during the course of the disease were acquired (Average CT scans per patient was 1.8, with a range from 1 to 6). The per-scan sensitivity and specificity for detecting COVID-19 in the independent test set was 114 of 127 (90% [95% confidence interval: 83%, 94%]) and 294 of 307 (96% [95% confidence interval: 93%, 98%]), respectively, with an AUC of 0.96. The details of their tests are given in **Table 1**.

In another study, a weakly-supervised deep learning-based software system was developed by Zheng et al. [46] using 3D CT volumes to detect COVID-19. The authors have searched unenhanced chest CT scans of patients with suspected COVID-19 from the picture archiving and communication system of radiology department (Union Hospital, Tongji Medical College, Huazhong University of

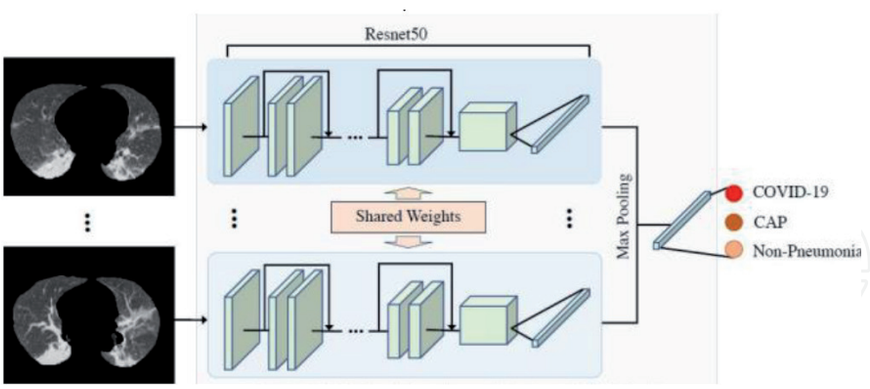


Figure 1.
COVID-19 detection neural network (COVNet) architecture [45].

	Sensitivity %	Specificity %	AUC
COVID-19	90 (114 of 127)	96 (294 of 307)	0.96
CAP	87 (152 of 175)	92 (239 of 259)	0.95
Non-Pneumonia	94 (124 of 132)	96 (291 of 302)	0.98

Note: Values in the parentheses are the numbers for the percentage calculations.

Table 1.
The performance of COVNet as per [45].

Science and Technology). 540 patients (age of 42.5 ± 16.1 years; range 3–81 years) were enrolled into the study, including 313 patients (age, 50.7 ± 14.7 years; range 8–81 years) with clinical diagnosed COVID-19 (COVID-positive group) and 227 patients (age of 31.2 ± 10.0 years; range, 3–69 years) without COVID-19 (COVID-negative group). As shown in **Figure 2**, the system takes a CT volume and its 3D lung mask as input, where the 3D lung mask is generated by a pre-trained U-Net. The proposed system is divided into three stages. The first stage consists of a 3D convolution with a kernel size of 5 × 7 × 7, a batchnorm layer and a pooling layer. The second stage is composed of two 3D residual blocks. In each one of the residual block, a 3D feature map is handed into both a 3D convolution with a batchnorm layer and a shorter connection containing a 3D convolution. The third stage is a progressive classifier, which contains three 3D convolution layers and a fully-connected layer with the softmax activation function. As described in **Figure 3**, a U-Net is trained for lung region segmentation on the labeled training set using the ground-truth lung masks generated by an unsupervised learning method. Then, the pre-trained U-Net is used to test all CT volumes to obtain the lung masks. The lung mask is concatenated with CT volume and serves as the input of the system. The authors have used the spatially global pooling layer and the temporally global pooling layer to technically handle the weakly-supervised COVID-19 detection problem.

Furthermore, Gozes et al. [47] presented a system that exploits 2D and 3D deep learning models. **Figure 4** shows a block diagram of the developed system. The system is comprised of several components and analyzes the CT case at two distinct levels: *Subsystem A and Subsystem B.* Subsystem A provides a 3D analysis of the case volume for nodules and focal opacities using existing, previously developed algorithms, where Subsystem B provides newly developed 2D analysis of each slice of

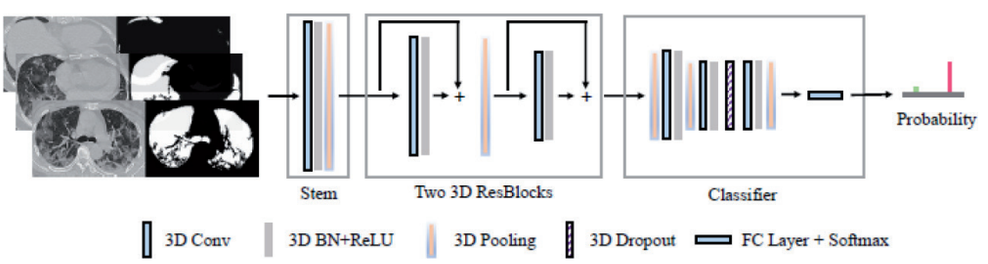


Figure 2.
The architecture proposed in [46]. The network takes a CT volume with its 3D lung mask as the input and outputs the probabilities of COVID-19 positive/negative.

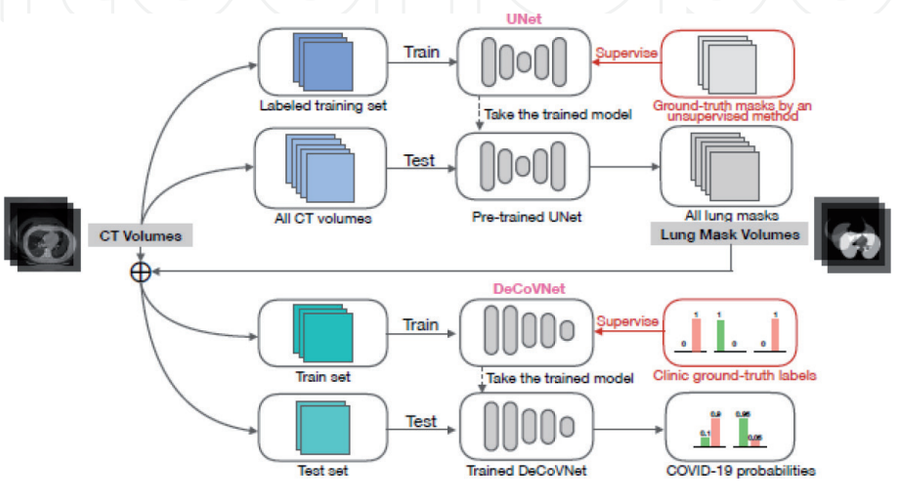


Figure 3.
Training and testing procedures [46].

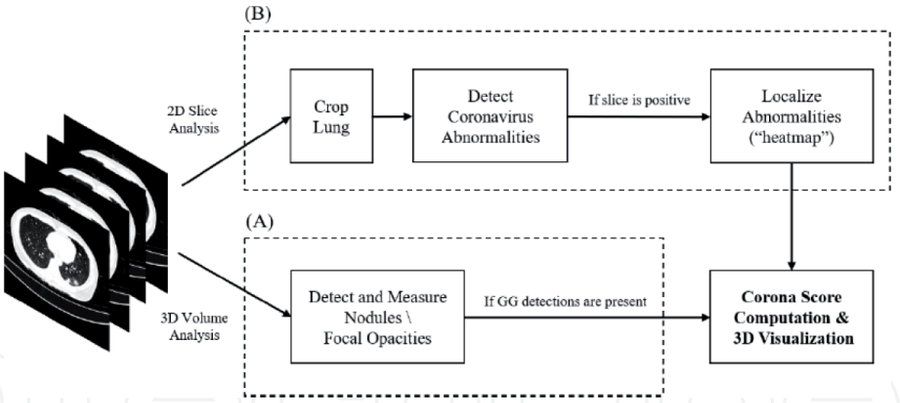


Figure 4.
System block diagram [47].

the case to detect and localize larger-sized diffuse opacities including ground glass infiltrates which have been clinically described as representative of Coronavirus. As argued by the authors, working in the 2D space has several advantages for deep learning based algorithms in limited data scenarios. These include an increase in the training samples (with many slices per single case), the ability to use pre-trained networks that are common in 2D space, and an easier annotation for segmentation purposes.

For Subsystem A, the authors used commercial off-the-shelf software that detects nodules and small opacities within a 3D lung volume. This software was developed as a solution for lung pathology detection and provides quantitative measurements (including volumetric measurements, axial measurements, calcification detection and texture characterization). For Subsystem B, the first step is the *lung crop stage*, where the lung region of interest is extracted using a lung segmentation module. In the following step, Coronavirus related abnormalities are detected using Resnet-50, which is a 2D CNN architecture that consists of 50 layers. In the classification stage, the authors calculated the ratio of positive detected slices out of the total slices of the lung (*positive ratio*). A positive case-decision is made if the positive ratio exceeds a pre-defined threshold. The system was tested on 157 patients from China and U.S. The sensitivity and the specificity of the system were 98.2% and 92.2%, respectively. **Figure 5** shows a patient case visualization.

The authors have also proposed a *Corona score* which is a volumetric measurement of the opacities burden. The corona score is computed by a volumetric summation of the network-activation maps. The system output enables quantitative measurements for smaller opacities (volume, diameter) and visualization of the larger opacities in a slice-based "heat map" or a 3D volume display. The authors claim that the score is robust to slice thickness and pixel spacing as it includes pixel volume. For patient-specific monitoring of disease progression, they suggested the *Relative Corona score* in which they normalize the corona score by the score computed at the first time point. The suggested "Corona score" measures the progression of disease over time. An example of such an implementation is shown in **Figure 6** which demonstrates a tracking over time of a specific opacity in a Coronavirus patient (red box). In this example, a patient was imaged in time points where the first CT scan was obtained few days following the first signs of the virus (fever, cough). This case involves multiple opacities and shows an overview of the patient recovery process with its corresponding Corona score over time.

Barstugan et al. [48] presented a classification system consisting of five different feature extraction methods followed by support vector machine (SVM). The feature extraction methods were Gray Level Co-occurrence Matrix (GLCM), Local

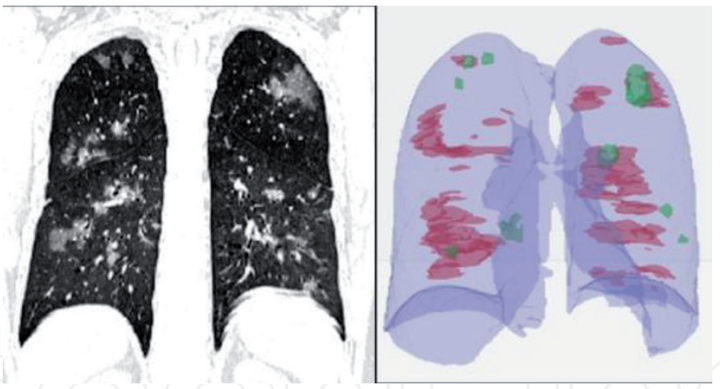


Figure 5.
Patient case visualization. Left: Coronal view; right: Automatically generated 3D volume map of focal opacities (green) and larger diffuse opacities (red) [47].

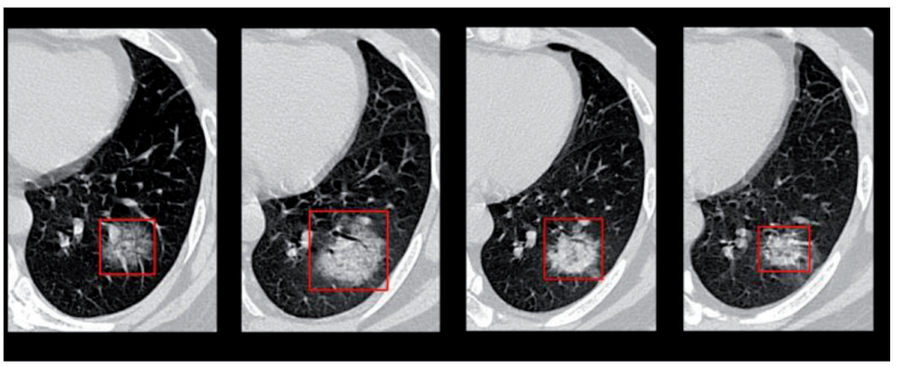


Figure 6.
Multi time point tracking of disease progression [47].

Directional Patterns (LDP), Gray Level Run Length Matrix (GLRLM), Gray Level Size Zone Matrix (GLSZM), and Discrete Wavelet Transform (DWT). To test the proposed system, four different datasets were formed by taking patches of size 16x16, 32x32, 48x48 and 64x64 from 150 CT images belonging to 53 infected cases, from the "Societa Italiana di Radiologia Medica e Interventistica". The samples of datasets were labeled as Coronavirus/non-Coronavirus (infected/non-infected). **Table 2** shows the four different subsets created from patch regions. The authors have implemented 2-fold, 5-fold and 10-fold cross-validations during the classification process. Sensitivity, specificity, accuracy, precision, and F-score metrics were used to evaluate the classification performance. **Figure 7** shows patch regions and patch samples from the four different subsets.

Caruso et al. [49] investigated chest CT features of patients with COVID-19 in Rome, Italy, and compared the diagnostic performance of CT with that of RT-PCR. All chest CT examinations were performed with patients in the supine position on a 128-slice CT scanner. Radiologists in consensus with thoracic imaging experience evaluated the images using a clinically available dedicated application (Thoracic VCAR, GE Medical Systems), defining patients as having positive CT findings when a diagnosis of viral pneumonia was reported. The study comprised 158 participants, of them fever was witnessed in 97 (61%) and cough and dyspnea were observed in 88 (56%) and 52 (33%), respectively. Of these patients, 62 (39%) had positive RT-PCR results and 102 (64%) had positive CT findings. Sensitivity, specificity, and accuracy of CT for COVID-19 pneumonia were 97% (60 of 62 participants), 56% (54 of 96 participants), and 72% (114 of 158 participants), respectively.

Table 3 details the CT features in participants with COVID-19 infection confirmed with RT-PCR as reported in [49]. The results presented in [49] agree with

Subset	Patch Dimension	Number of Non-Coronavirus Patches	Number of Coronavirus Patches
Subset 1	16 × 16	5912	6940
Subset 2	32 × 32	942	1122
Subset 3	48 × 48	255	306
Subset 4	64 × 64	76	107

Table 2.
Four different subsets created from patch regions [48].

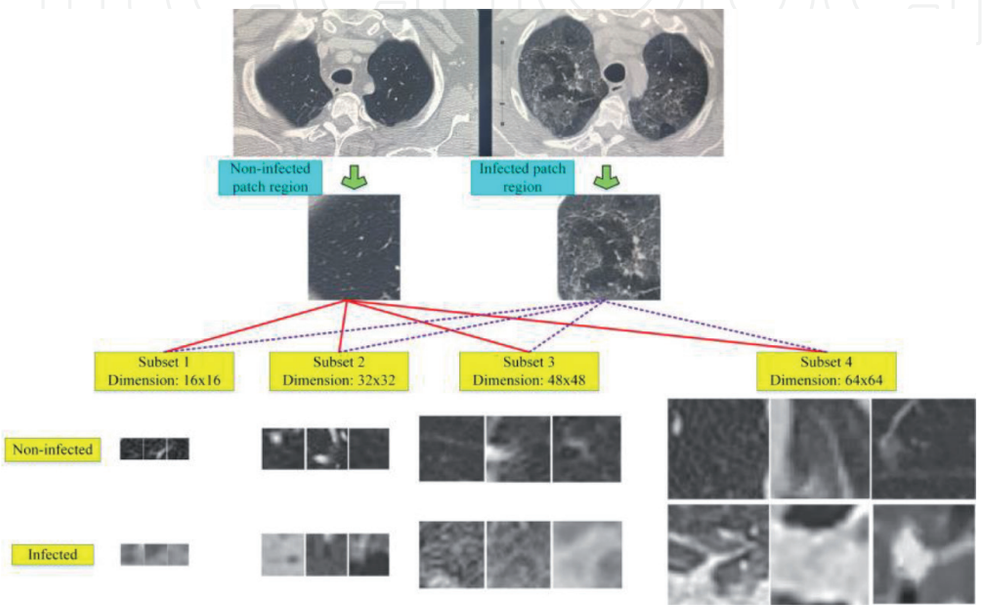


Figure 7.
Patch regions and patch samples from the four different subsets. Sample images for infected and non-infected situations for all subsets are shown as well [48].

the study performed by Salehi et al. [50] of 919 patients, despite some differences. However, the population in [50] varies from the population examined in [49]. Also, Chung et al. [51] analyzed a small population consisting of 21 patients and found a very low frequency of crazy paving pattern compared with [49] (19% vs. 39%).

Furthermore, Xu et al. [52] established a model to distinguish COVID-19 from influenza-A viral pneumonia (IAVP) and healthy cases through pulmonary CT images. The authors have discussed that the RT-PCR detection of viral RNA from sputum or nasopharyngeal swab have a relatively low positive rate in the early stage. They argued that the manifestations of COVID-19 as seen through CT imaging show individual characteristics that differ from those of other types of viral pneumonia such as IAVP. The suggested model consists of multiple CNNs, where the candidate infection regions are segmented out from the pulmonary CT image set. Then, these separated images are categorized into the COVID-19, IAVP, and irrelevant to infection groups, together with the corresponding confidence scores, using a location-attention classification model. Finally, the infection type and overall confidence score for each CT case are calculated using the Noisy-OR Bayesian function.

Figure 8 shows the whole process. As described in the figure, the CT images are first preprocessed to excavate the effective pulmonary regions. Then, a 3D CNN segmentation model is used to segment multiple candidate image cubes. After that, an image classification model is used to classify all the image patches into three

CT Feature	No. of Participants (n = 58)	Percentage
GGO	58	100
Multilobe involvement (≥2 lobes)	54	93
Bilateral distribution	53	91
Posterior involvement	54	93
GGO location (peripheral)	52	89
Subsegmentel vessel enlargement (>3 mm)	52	89
Consolidation	42	72
Subsegmental	32	55
Segmental	10	17
Lymphadenopathy	34	58
Bronchiectasis	24	41
Air bronchogram	21	36
Pulmonary nodules surrounded by GGO	10	17
Interlobular septal thickening	8	13
Halo sign	7	12
Pericardial effusion	3	5
Pleural effusion	2	3
Bronchial wall thickening	1	1
Cavitation	0	0

Table 3.
CT features in participants with COVID-19 infection confirmed with RT-PCR [49].

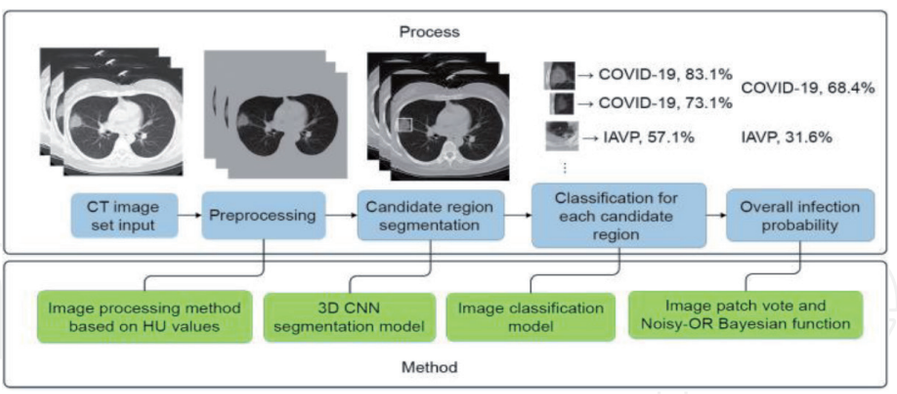


Figure 8.
The process flow chart of [52].

kinds: COVID-19, IAVP, and irrelevant to infection. Image patches from the same group "vote" for the type and confidence score of this candidate as a whole. Finally, the Noisy-OR Bayesian function is used to calculate the overall analysis report for one CT sample. It is worth mentioning that the model uses a V-Net as the backbone feature extraction part. The authors have further discussed how the variable 3D structures of the lesion regions can aggravate the results. For example, when the border between a healthy region and the infected one becomes blurred and indistinct, it will be difficult to label pixel-level masks for lesion regions of pneumonia. As such, the model uses the RPN structure [52] to capture the region of interest with 3D bounding boxes instead of pixel-level segmented masks.

To evaluate the system, two classification models were used, as shown in **Figure 9**. The first one was the ResNet model and the other was designed based on the first network structure by concatenating the location-attention mechanism in the full-connection layer to improve the overall accuracy rate. The resultant model was added to the first full-connection layer to enhance the influence of this factor on the whole network. The output of the convolution layer was flattened to a 256-dimensional feature vector and then converted into a 16-dimensional feature vector using a full-connection network. The overall accuracy rate was 86.7% in terms of all the CT cases taken together.

Belfiore et al. [53] presented a practice of a good tool for radiologists (Thoracic VCAR) that can be used in COVID-19 diagnosis. Thoracic VCAR offers quantitative measurements of the lung involvement. Further, it can generate a clear, fast and concise report that communicates vital medical information to referring physicians. In the post-processing phase, the software can recognize the ground glass and differentiate it from consolidation and quantifies them as a percentage with respect to the healthy parenchyma. This information is useful for evaluating regression or progression disease in response to drug therapy as well as evaluating the effectiveness of pronation maneuvers for alveolar recruitment in ICU patients. The authors in [53] have discussed the importance of such high-resolution CT (HRCT) technique in investigating the patients with suspicion COVID-19 pneumonia. They have argued that the HRCT is a very accurate technique in identifying pathognomic findings of interstitial pneumonia as ground glass areas, crazy paving, nodules and consolidations, mono- or bilateral, patchy or multifocal, central and/or peripheral distribution, declivous or nondeclivous. As per the discussion, during the follow-up, HRCT examination can quantify the course of the disease and evaluate the effectiveness of the experimental trial and the patient's prognosis.

In [54], Mei et al. have also used AI algorithms to integrate chest CT findings with clinical symptoms, exposure history and laboratory testing to rapidly diagnose patients who are positive for COVID-19. Among a total of 905 patients

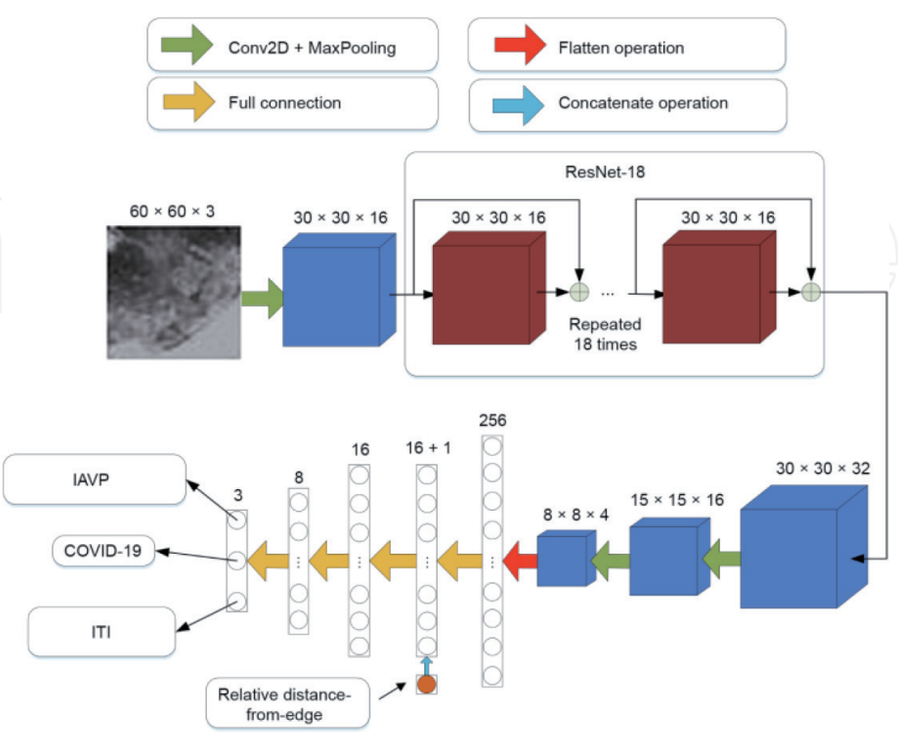


Figure 9.
The network structure of ResNet-18-based classification model [52].

tested by real-time RT–PCR test, 419 (46.3%) tested positive for SARS-CoV-2. In this study, the dataset included patients aged from 1 to 91 years (with mean of 40.7 year and standard deviation of 6.5 years) where 488 of the patients were men and 417 were women. All scans were acquired using a standard chest CT protocol and were reconstructed using the multiple kernels and displayed with a lung window. Clinical information included travel and exposure history, leukocyte counts (including absolute neutrophil number, percentage neutrophils, absolute lymphocyte number and percentage lymphocytes), symptomatology (presence of fever, cough and sputum), patient age and patient sex. More specifically, the authors developed a CNN to learn the imaging characteristics of patients on the initial CT scan. They used multilayer perceptron classifiers to classify patients with COVID-19 according to the radiological data and clinical information.

Of the 134 positive cases in the test set, 90 were correctly categorized by both the joint model and the senior thoracic radiologist and 33 were classified differently. Of the 33 patients, 23 were correctly classified as positive by the joint model, but were misclassified by the senior thoracic radiologist. Ten patients were classified as negative by the joint model, but correctly diagnosed by the senior thoracic radiologist. Eleven patients were misclassified by both the joint model and the senior thoracic radiologist. Of the 145 patients negative for COVID-19 in the test set, 113 were correctly classified by both the joint model and the senior thoracic radiologist. Thirty-two out of 145 were classified differently by the joint model and the senior thoracic radiologist. Seven were correctly classified as negative by the joint model, but were diagnosed as positive by the senior thoracic radiologist. Twenty-three were classified as positive by the joint model, but correctly diagnosed as negative by the senior thoracic radiologist. Two patients were misclassified by both the joint model and the senior thoracic radiologist. As discussed in [54], patient's age, presence of exposure to SARS-CoV-2, presence of fever, cough, cough with sputum, and white blood cell counts are significant features associated with SARS-CoV-2 status. However, it should be pointed out that difficulties on model training have been witnessed due to the limited sample size.

Moreover, Fei et al. [55] developed a deep learning-based system for automatic segmentation of lung and infection sites using chest CT. Likewise, Xiaowei et al. [56] distinguished COVID-19 pneumonia and Influenza-A viral pneumonia from healthy cases. Further, Shuai et al. [57] developed a system to extract the graphical features in order to provide a clinical diagnosis before pathogenic testing and thus save critical time. Also, Zheng et al. [58] developed a model for automatic detection using 3D CT volumes. Bai et al. [59] established and evaluated an AI system for differentiating COVID-19 and other pneumonia from chest CT to assess radiologist performance. As they have discussed, distinguishing COVID-19 from normal lung or other lung diseases, such as cancer from chest CT, may be straightforward. However, a major difficulty in controlling the current pandemic is making out subtle radiologic differences between COVID-19 and pneumonia of other origins. A total of 521 patients with positive RT-PCR results for COVID-19 and abnormal chest CT findings were retrospectively identified from 10 hospitals. A total of 665 patients with non–COVID-19 pneumonia and definite evidence of pneumonia from chest CT were retrospectively selected from three hospitals.

Further, the authors have performed data augmentation dynamically during training and included flips, scaling, rotations, random brightness and contrast manipulations, random noise, and blurring. Training was performed for 20 epochs, where each epoch was defined as 16000 slices. A classification model was trained to distinguish between slices with and those without pneumonia-like findings

(both COVID-19 and non–COVID-19). In more technical details, the EfficientNet B4 architecture was used for the pneumonia classification task. Each slice was stacked to three channels as the input of EfficientNet that used pretrained weights on ImageNet. EfficientNets with dense top fully connected layers were used. There were four fully connected layers of 256, 128, 64, and 32 neurons, respectively. Also, a fully connected layer with 16 neurons with batch normalization and a classification layer with sigmoid activation were added at the end of EfficientNet. Then, the slices were pooled using a two-layer fully connected neural network to make predictions at the patient level. **Figure 10** shows the proposed classification neural network model, while **Figure 11** demonstrates the model's flowchart.

Kumar et al. [60] proposed a framework that collects a big amount of data from various hospitals and trains a deep learning model over a decentralized network using the most recent information related to COVID-19 patients based on CT slices. The authors suggested the integration of blockchain and federated-learning technology that allow the collection of data from different hospitals without the leakage of data; a step that adds the necessary privacy to the model. They employed Google's Inception V3 network for feature extraction and tested various learning models (VGG, DenseNet, AlexNet, MobileNet, ResNet, and Capsule Network) in order

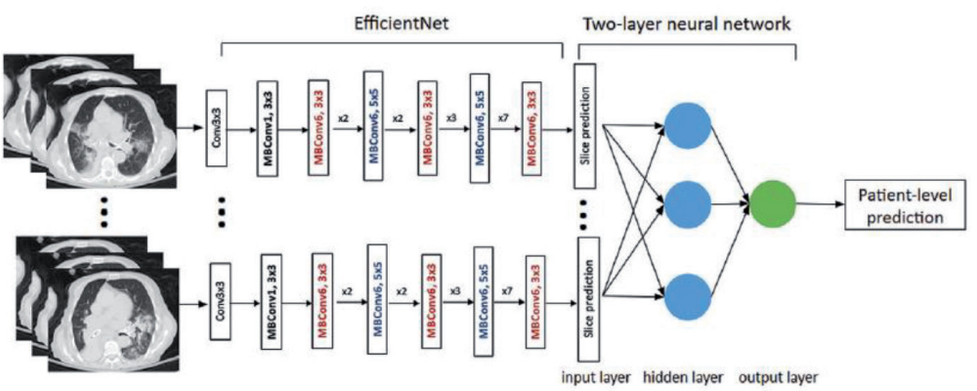


Figure 10.
Classification neural network model proposed by [59].

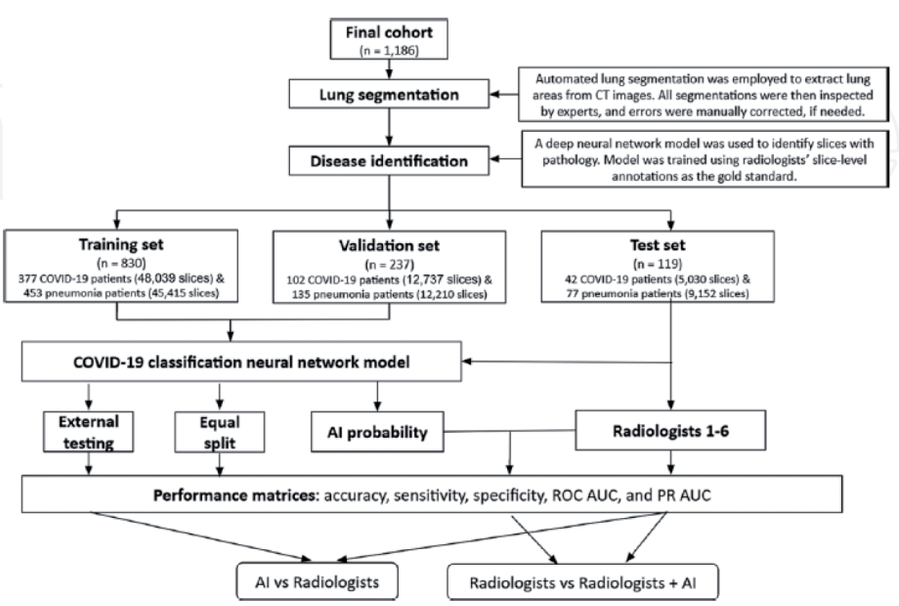


Figure 11.
The flowchart showing the AI model used to distinguish COVID-19 from non–COVID-19 pneumonia. (PR AUC = precision recall area under curve, ROC AUC = receiver operator characteristics area under the curve) [59].

to recognize the patterns from lung screening. They found that Capsule network achieved the best performance when compared to other learning models. **Figure 12** shows the suggested model in [60].

The Capsule network contains four layers: i) Convolutional layer, ii) Hidden layer, iii) PrimaryCaps layer, and iv) DigitCaps layer. A capsule is made when input features are in the lower layer. Each layer of the Capsule Network contains many capsules. To train it, the activation layer represents the parameters of the entity and computes the length of the Capsule network to re-compute the scores of the feature part. The capsule acts as a neuron. Capsule networks tend to describe an image at a component level and associate a vector with each component. The probability of the existence of a component is represented by the vectors lengths.

In federated learning, the hospitals keep their data private and share only the weights and gradients while blockchain technology is used to distribute the data securely among the hospitals. Federated learning was proposed by McMahan et al. [61] to learn from the shared model while protecting the privacy of data. In this context, the federated learning is used to secure data and aggregate the parameters from multiple organizations. As argued by the authors, since the volume of data is big, placing them on the blockchain directly with its limited storage space will be very expensive and resource-intensive. As such, a special data manipulation is needed. So, the hospital needs to store a transaction in the block to verify the ownership. The hospital data include the data type and size. It is noteworthy that federated learning does not affect the accuracy but it adds the privacy while sharing the data. Some selected 3D samples from the dataset are shown in **Figure 13**. The authors have claimed that the system sensitivity is 0.96, and its precision is 0.83. However, its specificity was not very attractive.

A simple 2D deep learning framework was developed in [62] to diagnose COVID-19 pneumonia based on a single chest CT image using transfer learning. For training and testing, the authors collected 3993 chest CT images of patients with COVID-19 pneumonia, other pneumonia and nonpneumonia diseases. These CT images were split into a training set and a testing set at a ratio of 8:2. After a simple preprocessing stage, three channels (256 × 256 × 3 pixels) were arranged in the input layer and fed into the pretrained model layers. In the pre-trained model layers, the authors included one of these four models (VGG16, ResNet-50, Inception-v3, and Xception). Each model comprises two parts: a convolutional base and a classifier. The convolutional base is composed of a stack of convolutional and pooling layers to generate features from the images. The role of the classifier is to categorize the image based on the extracted features. The activations from the pretrained model layers were fed into the additional layers. In the additional layers, the activations were first flattened and connected to two fully connected layers: one consisted of 32 nodes, and the other consisted of three nodes. Subsequently, the activations from the second fully connected layer were fed into a SoftMax layer, which provided the probability for each of the

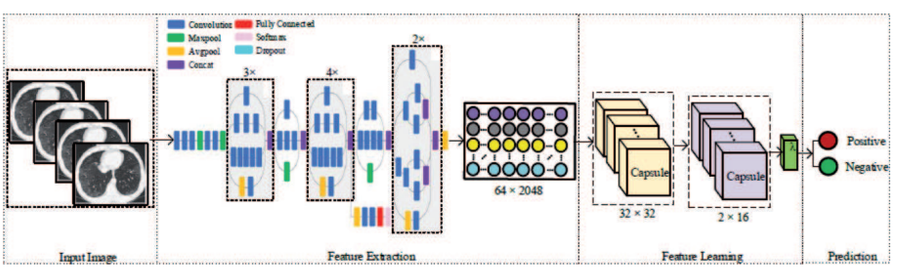


Figure 12.
COVID-19 model suggested by [60].

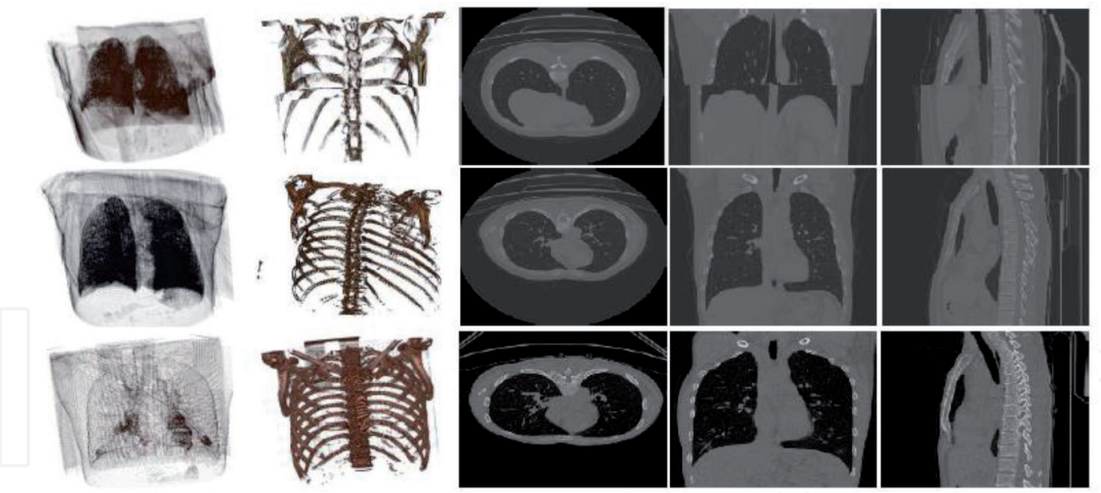


Figure 13.
Selected samples from [60].

classes (COVID-19, other pneumonia, and nonpneumonia). However, the study has several limitations as well. First, the testing dataset was obtained from the same sources as the training data set. This may raise issues of generalizability and overfitting of the models. Indeed, the authors have mentioned that the detection accuracy decreased when datasets from other published papers were used.

Song et al. [63] first extracted the main regions of the lungs and filled the blank of lung segmentation with the lung itself to avoid noise caused by different lung contours. Then, they extracted the top-K details in the CT images and obtained image-level predictions. Finally, the image-level predictions were combined to attain patient-level diagnoses. In the testing set, the model achieved an AUC of 0.95 and sensitivity of 0.96. In [64], Jin et al. built a method to accelerate the diagnosis speed. This model was trained using 312 images. Yet, it achieved a comparable performance with experienced radiologists. Among 1255 independent testing cases, the proposed deep-learning model achieved an accuracy of 94.98%, an AUC of 97.91%, a sensitivity of 94.06% and a specificity of 95.47%.

Zheng et al. [65] used U-Net to segment the lung area automatically, and then used 3DResNet for classification. As they have discussed, infectious areas can be distributed in many locations in the lungs, and automatic infectious area detection may not guarantee very high precision. Consequently, using the whole lung for classification is more convenient in practice. In [66], 3506 patients (468 with COVID-19, 1551 with CAP, and 1303 with non-pneumonia) were used to train and test another deep-learning model. The authors first used U-net to extract the whole lung region as an ROI. Afterwards, 2D RestNet50 was used for classifying COVID-19. Since each CT scanning includes multiple 2D image slices, the features in the last layer of ResNet50 were max pooled and combined for prediction. The model achieved an AUC of 0.96 in classifying COVID-19 from CAP and other pneumonia. Moreover, Shi et al. [67] included 1658 patients with COVID-19 and 1027 patients with CAP for classification. They first used VBNet to segment the infected areas, bilateral lungs, 5 lung lobes, and 18 lung pulmonary areas. Then, hand-crafted features such as location specific features, infection size, and radiomic features were extracted, and least absolute shrinkage and selection operator (LASSO) was used for feature selection. The method reached sensitivity of 0.9, specificity of 0.8, and accuracy of 0.88.

Further, Dong et al. [68] reviewed the use of various imaging characteristics and computing models that have been applied for the management of COVID-19. Specifically, they have quantitatively analyzed the use of imaging data for detection

and treatment by means of CT, positron emission tomography - CT (PET/CT), lung ultrasound, and magnetic resonance imaging (MRI). PET is a sensitive but invasive imaging method that plays an important role in evaluating inflammatory and infectious pulmonary diseases, monitoring disease progression and treatment effect, and improving patient management. It is worth mentioning that lung ultrasound is a non-invasive, radiation-free, and portable imaging method that allows for an initial bedside screening of low-risk patients, diagnosis of suspected cases in the emergency room setting, prognostic stratification, and monitoring of the changes in pneumonia [69, 70].

Also, Jin et al. [71] presented their experience in building and deploying an AI system that analyzes CT images and detects COVID-19 pneumonia features. They obtained the image samples from five different hospitals with 11 different models of CT equipment to increase the model's generalization ability. The combined "segmentation - classification" model pipeline, can highlight the lesion regions in addition to the screening result. The model pipeline is divided into two stages: 3D segmentation and classification. The pipeline leverages a model library that contains different segmentation models such as FCN-8 s, U-Net, V-Net, and 3D U-Net++, as well as the classification models like dual path network (DPN-92), Inception-v3, ResNet-50, and Attention ResNet-50. As for the training set, in addition to the positive cases, they assembled a set of negative images of inflammatory and neoplastic pulmonary diseases, such as lobar pneumonia, lobster pneumonia, and old lesions. Their aim was enabling the model to learn different COVID-19 features from various resources. Using 1136 training cases (723 positives for COVID-19), they were able to achieve a sensitivity of 0.974 and a specificity of 0.922 on the test set. Further, the system achieved an AUC of 0.991. According to the authors, the system is in use in 16 hospitals and has a daily capacity of over 1300 screenings. Similarly, Jin et al. [72] performed an extensive statistical analysis on CT images diagnosed by COVID-19.

They evaluated the system on a large dataset with more than 10000 CT volumes from COVID-19, influenza-A/B, non-viral CAP and non-pneumonia subjects. **Figure 14** shows the workflow of the suggested system. The system consists of five key parts: (1) lung segmentation network, (2) slice diagnosis network, (3) COVID-infectious slice locating network, (4) visualization module for interpreting the vital region, and (5) image phenotype analysis module for features explanation. CT volumes were divided into different cohorts. The authors claimed that the system achieved an AUC of 97.81% on a test set of 3199 scans.

Jin et al. [73] drafted a guideline according to the guidelines methodology and general rules of WHO in relation to CT imaging. This guideline includes the epidemiological characteristics, disease screening, diagnosis, treatment, and nosocomial infection prevention. In this regard, the authors have discussed that the imaging findings vary with the patient's age, immunity status, disease stage at the time of scanning, underlying diseases, and drug interventions. The imaging features of lesions show: (1) dominant distribution (mainly subpleural, along the bronchial vascular bundles), (2) quantity (often more than three or more lesions, occasional single or double lesions), (3) shape (patchy, large block, nodular, lumpy, honeycomb-like or grid-like, cord-like, etc.), (4) density (mostly uneven, a paving stones-like change mixed with ground glass density and interlobular septal thickening, consolidation and thickened bronchial wall, etc.), and (5) concomitant signs variations (air-bronchogram, rare pleural effusion and mediastinal lymph nodes enlargement, etc.).

In addition, Chen et al. [74] constructed a system based on deep learning for detecting COVID-19 pneumonia from high resolution CT. For model development and validation, 46096 anonymous images from 106 admitted patients, including 51

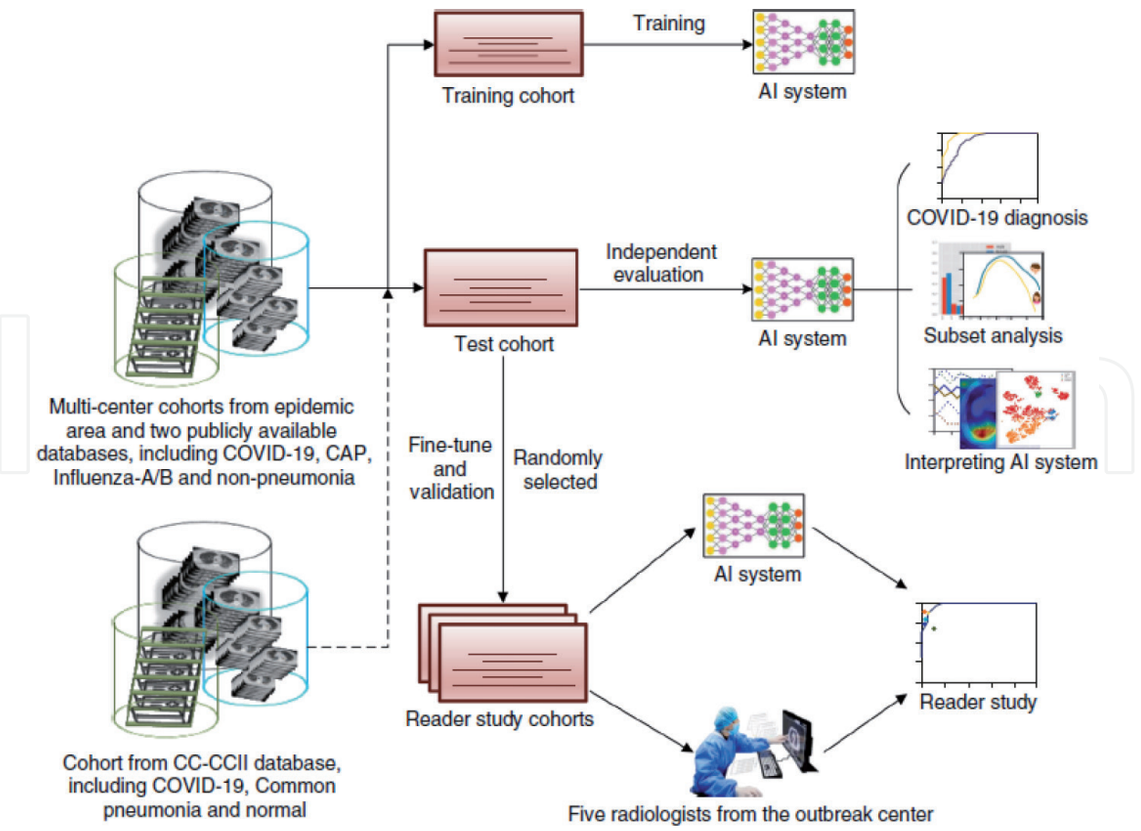


Figure 14.
The workflow of the AI system suggested in [72].

patients of laboratory confirmed COVID-19 pneumonia and 55 control patients of other diseases in Renmin Hospital of Wuhan University were retrospectively collected and processed. Twenty-seven consecutive patients who underwent CT scans were prospectively collected to evaluate and compare the efficiency of radiologists against COVID-19 pneumonia with that of the model. The authors have first filtered the images where 35355 images were selected and split into training and testing datasets. In more detail, the authors implemented UNet++ being a well-known architecture for medical image segmentation. They trained UNet++ to extract valid areas in CT images using 289 randomly selected CT images and tested it on other 600 randomly selected CT images. The training images were labeled with the smallest rectangle containing all valid areas. With the raw CT scan images taken as the input, and the labeled map from the expert as the output, UNet++ was used to train in an image-to-image manner. The model successfully extracted valid areas in 600 images from the testing set with an accuracy of 100%. Based on system performance, the authors constructed a cloud-based platform to provide a worldwide assistance for detecting COVID-19 pneumonia [75].

In [76], Vinod and Prabaharan have elaborated a methodology that helps identifying COVID-19 infected people among the normal individuals by utilizing CT scan. The image diagnosis tool utilizes decision tree classifier for finding Coronavirus infected person. The percentage accuracy of an image was analyzed in terms of precision, recall score and F1 score. Moreover, Gieraerts et al. [77] hypothesized that the use of semi-automated AI may allow for more accurate patient detection. They assessed COVID-19 patients who underwent chest CT by conventional visual and AI-based quantification of lung injury. They also studied the impact of chest CT variability in determining the potential response to novel antiviral therapies. In their study, 250 consecutive patients with clinical suspicion of COVID-19 pneumonia were tested with both RT-PCR and CT within a 2-hour

interval of hospital admission. Epidemiological, demographic, clinical, and laboratory data at admission were obtained from the electronic patient management system.

In Zhang et al. [78], 4695 manually annotated CT slices were used to build seven classes, including background, lung field, consolidation, ground-glass opacity, pulmonary fibrosis, interstitial thickening, and pleural effusion. After a comparison between different semantic segmentation approaches, the authors selected DeepLabv3 as the segmentation detection backbone. The diagnostic system was based on a neural network fed by the lung-lesion maps. The results showed a COVID-19 diagnostic accuracy of 92.49% when tested on 260 subjects. In Bai et al. [79], a direct classification of COVID-19 specific pneumonia versus other etiologies was performed using an EfficientNet B5 network followed by a two-layer fully connected network to pool the information from multiple slices and provide a patient-level diagnosis. This system yielded 96% accuracy on a testing set of 119 subjects compared to an average accuracy of 85% for six radiologists.

Also, Ying et al. [80] used 2D slices including lung regions segmented by OpenCV. Fifteen slices of complete lungs were derived from each 3D chest CT images, and each 2D slice was used as the input to the system. A pretrained ResNet-50 was used and the Feature Pyramid Network (FPN) was added to extract the top-K details from each image. An attention module was coupled to learn the important details. Chest CT images from 88 patients with COVID-19, 101 patients with bacterial pneumonia, and 86 healthy persons were used. The model achieved an accuracy of 86% for pneumonia classification (COVID-19 or bacterial pneumonia), and an accuracy of 94% for pneumonia diagnosis (COVID-19 or healthy). Wang et al. [81] used 1065 chest CT scan images of COVID-19 patients to build a classifier using InceptionNet. They reported an accuracy of 89.5%, a specificity of 0.88, and a sensitivity of 0.87. In [82], different deep learning approaches (VGG16, InceptionResNetV2, ResNet50, VGG19, MobilenetV2, and NasNetMobile) have been modified and tested on 400 CT scan images. The results have shown that NasNetMobile outperformed all other models in terms of accuracy (81.5% –95.2%). On the other hand, Mucahid et al. [83] used classical feature extraction techniques for COVID-19 detection. For example, they have implemented gray level co-occurrence matrices (GLCM), local directional pattern (LDP), gray-level run length matrix (GLRLM), and discrete wavelet transform (DWT). They reported an accuracy of 99.68% in the best configuration settings.

Modegh et al. [84] proposed a system to distinguish healthy people, patients with COVID-19, and patients with other pneumonia diseases from axial lung CT-scan images. The general workflow for the proposed model is shown in **Figure 15**. The Ground Glass Opacity Axial (GGOA) CT-scan images are preprocessed and the lobes of the lungs are detected and extracted from the axial slices. The images of the left and right lobes of all the slices are then fed into two deep CNNs, one for calculating the probability of being diseased versus healthy, and the other for calculating the probability of diagnosis to be COVID-19 versus other diseases. In addition, the system detects the infected areas in the lung images. At the end, the probabilities assigned to the lobes are aggregated to make a final decision.

Figure 16 shows the model used for calculating the probability of each slice lobe being infected. The model was evaluated on a dataset of 3359 samples from 6 different medical centers and achieved sensitivities of 97.8% and 98.2%, and specificities of 87% and 81% in distinguishing normal cases from the diseased and COVID-19 from other diseases, respectively. Authors in [85] examined the effect of generalizability of the deep learning models, given the heterogeneous factors in training datasets such as patient demographics and pre-existing clinical conditions. The examination was done by evaluating the classification models trained to identify COVID-19 positive patients on 3D CT datasets from different

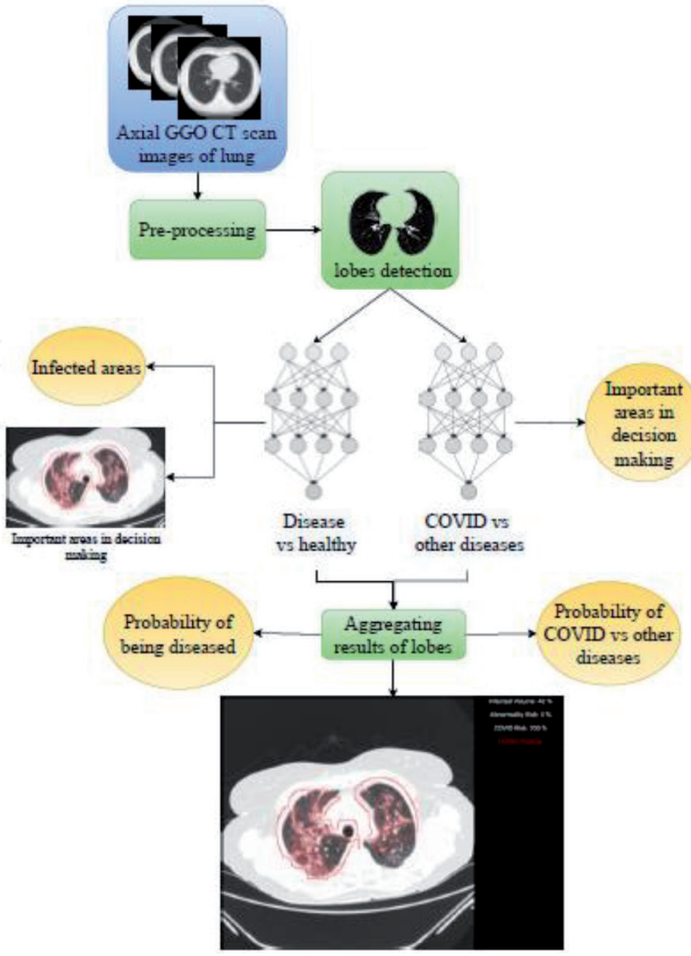


Figure 15.
The general workflow for the interpretable COVID-19 detection proposed in [84].

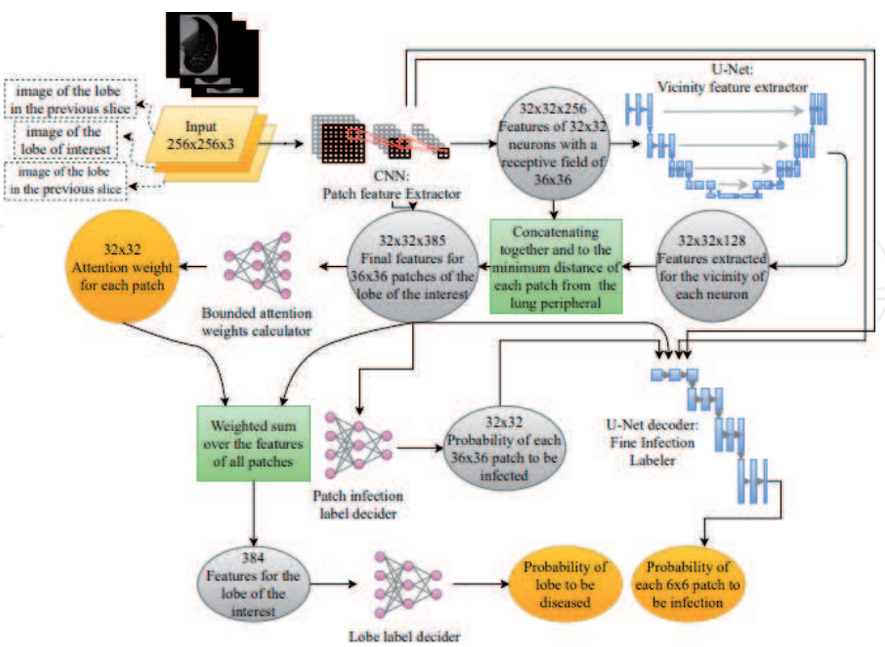


Figure 16.
The deep model used for calculating the probability of each slice lobe [84].

countries: UT Southwestern (UTSW), CC-CCII Dataset (China), COVID-CTset (Iran), and MosMedData (Russia). The data were divided into two classes: COVID-19 positive and COVID-19 negative patients. The models trained on a

single dataset achieved accuracy/AUC values of 0.87/0.826 (UTSW), 0.97/0.988 (CC-CCCI), and 0.86/0.873 (COVID-CTset) when evaluated on their own dataset.

In addition, Shah et al. [86] developed a deep learning network (CTnet-10) for COVID-19 classification. The model is fed with an input image of size 128 × 128 × 3. It passes through two convolutional blocks of dimensions 126 × 126 × 32, 124 × 124 × 32 respectively. Then it passes through a max-pooling of dimension 62 × 62 × 32 followed by two convolutional layers of dimensions 60 × 60 × 32, 58 × 58 × 32 respectively. Then, it is passed through a pooling layer of dimension 29 × 29 × 32, a flattened layer of 26912 neurons, and dropout layers of 256 neurons. After that, it is passed through a dense layer of a single neuron, where the CT scan image is classified as COVID-19 positive or negative. The system achieved an accuracy of 82.1%. The CTnet-10 model architecture is shown in **Figure 17**.

VB-Net, a deep learning network, was developed by Shan et al. [87] to quantify longitudinal changes in the follow-up CT scans of COVID-19 patients, and to explore the quantitative lesion distribution. VB-Net is a modified 3D CNN that consists of two paths. The first is a contracting path including down-sampling and convolution operations to extract global image features. The second is an expansive path including up-sampling and convolution operations to integrate fine-grained image features. Compared with V-Net, the VB-Net is much faster. The system not only performs auto-contouring of infection regions, but also accurately estimates their shapes, volumes and percentage of infection (POI) in CT scans. In addition, it measures the severity of COVID-19 and the distribution of infection within the lung. The accurate segmentation provides quantitative information that is necessary

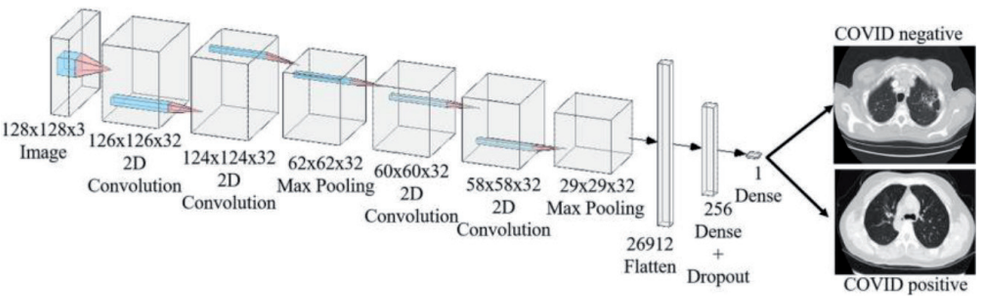


Figure 17.
CTnet-10 model architecture [86].

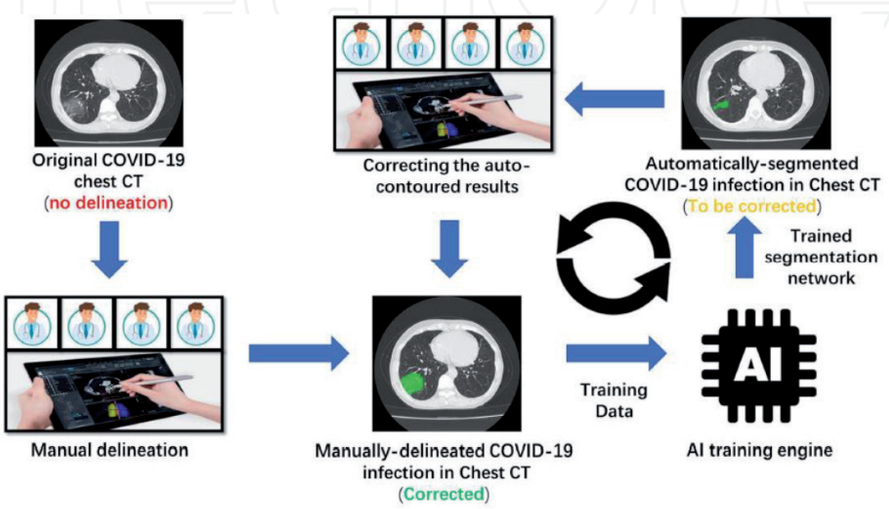


Figure 18.
The human-in-the-loop workflow [87].

to track disease progression and analyze longitude changes of COVID-19 during the entire treatment period. After segmentation, various metrics are computed to quantify the infection, including the volumes of infection in the whole lung, and the volumes of infection in each lobe and each bronchopulmonary segment.

The system was trained using 249 COVID- 19 patients, and validated using 300 new COVID-19 patients. To accelerate the manual delineation of CT images for training, a human-in-the-loop (HITL) strategy (shown in **Figure 18**) was adopted to assist radiologists to refine automatic annotation of each case. To evaluate the performance of the system, the Dice similarity coefficient, the differences of volume and the POI were calculated between the automatic and the manual

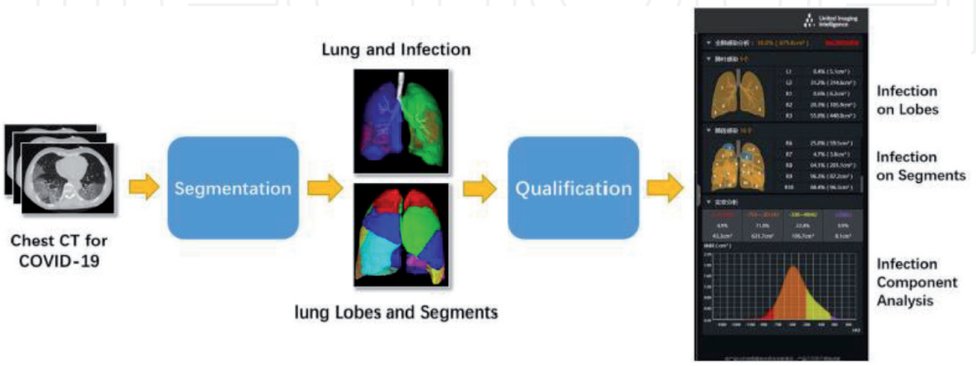


Figure 19.
The proposed pipeline for quantifying COVID-19 infection [87].

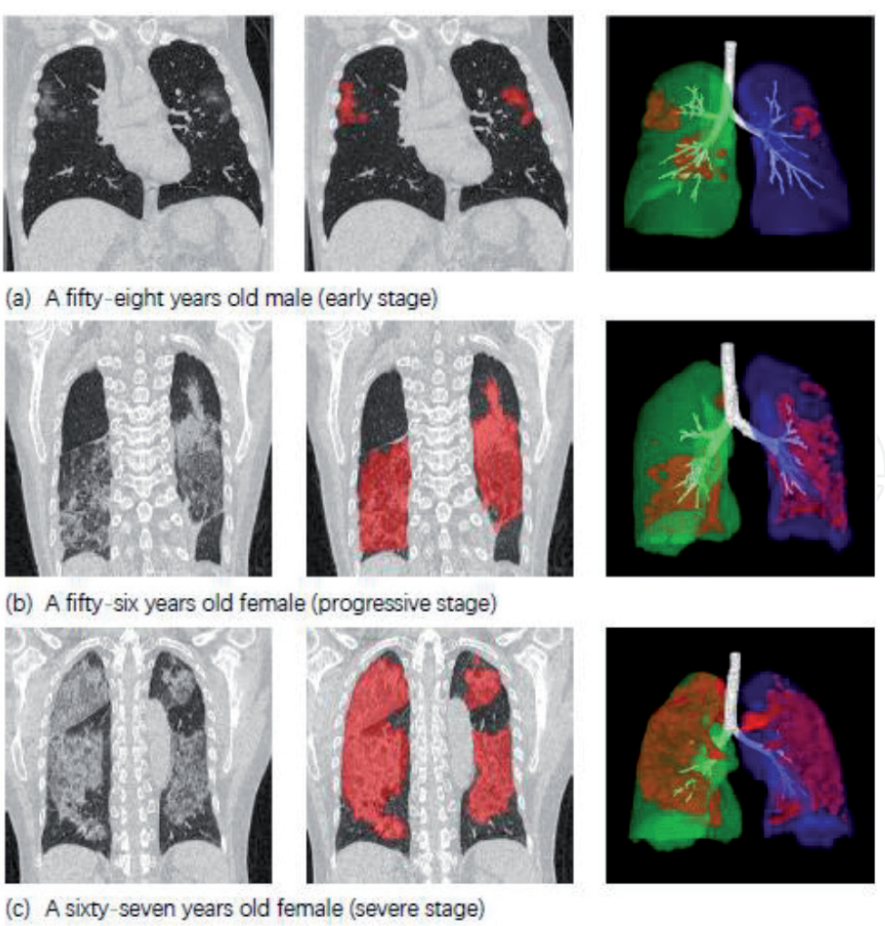


Figure 20.
Typical infection segmentation results of CT scans for three COVID-19 patients. Rows 1–3: Early, progressive and severe stages. Columns 1–3: CT image, CT images overlaid with segmentation, and 3D surface rendering of segmented infections [87].

segmentation results on the validation set. The system yielded a Dice similarity coefficient of 91.6% and a mean POI estimation error of 0.3% for the whole lung on the validation dataset. Moreover, the proposed HITL strategy reduced the delineation time to 4 minutes after 3 iterations of model updating, compared to the cases of fully manual delineation that often take 1 to 5 hours. **Figure 19** shows the pipeline for quantifying COVID-19 infection, whereas **Figure 20** shows typical infection segmentation results of CT scans for three COVID-19 patients.

4. Discussion

The specific nature of COVID-19 pandemic requires strong coordination of connected data, people, and systems to facilitate worldwide collaboration in fighting against it. From this study, we notice that healthcare stakeholders are not using the same systems, data formats, or standards. This can obstruct the ability to identify the possible trends of solutions to the pandemic related challenges and develop interventions among the associated efforts. Public health researchers, epidemiologists, and government officials need to be connected via integrated systems with connected data to understand the evolving pandemic better and make collective decisions on addressing this crisis. An important key action that needs to be taken to ensure best possible fight of the current (or even future) pandemic(s) is to catalyze scaling up the implementation of AI and ML in health sector.

Our study specifically suggests the following important issues that need to be addressed intensely and more efficiently:

- Due to the low contrast of the infection regions in some images and large variation of both shape and position across different patients, delineating the infection regions from the chest images is very challenging [88, 89]. Researchers are challenged to investigate AI techniques that may help in this direction.

- Although CT provides rich pathological information, it was noticed that in some cases only qualitative evaluation has been provided and precise changes across follow-up CT scans are often ignored. Actually, contouring infection regions in the Chest CT is necessary for quantitative assessment [90, 91]. As such, more investigation is required in this area.

- Quantifying imaging metrics and correlating them with syndromes, epidemiology, and treatment responses is essential and could further reveal insights about imaging markers and findings toward improved diagnosis and treatment for COVID-19 [92, 93].

- Some segmentation models were trained using imperfect ground-truth data. This could be improved by using 3D segmentation networks and adopting precise ground-truth annotated by experts [94, 95].

- The images in some datasets were acquired from different devices. This situation makes the classification process a kind of challenging. This could be explained by the fact that some gray-levels in one image represent certain Coronavirus infected levels, and the same gray-levels in another image may represent different levels (may lead to different decisions) [96, 97].

- Some systems were developed to quantify infections only, and it may not be applicable for quantifying other pneumonia, for example bacterial pneumonia [98, 99].

- Many datasets were collected in one center, which may not be representative of all COVID-19 patients in other geographic areas. The generalization of the deep learning system needs to be further validated on multi-center datasets [100].

- Experimental evidence is presented on datasets of hundreds (maybe thousands). However, the need is to go to real world settings, in which databases consist of hundreds of thousands and even more cases, with large variability [101].

5. Conclusion

The COVID-19 is a disease that has spread all over the world. This work attempted to provide a detailed study on how the AI and ML can help in various domains related to COVID-19, specifically in the area of disease diagnosis using CT imagery. In pursuing so, we considered, examined, discussed, and analyzed comprehensive studies and detailed researches proposed by intellectuals and researchers from various scientific communities and international academic institutions. Deep learning techniques and algorithms have shown immense appearances and implementations in different domains and COVID-19 related applications.

AI solutions have the potential to detect and analyze any abnormalities in health conditions in general, and related to COVID-19 in particular. The study has demonstrated that AI solutions can assist in differentiating Coronavirus patients from those who do not have the disease and can provide support in tracking disease progression. AI technology can potentially support radiologists in the triage, quantification, and trend analysis of data. For example, if the developed technique suggests a significantly increased likelihood of disease, then the case can be flagged for further review by a radiologist or clinician for possible treatment/quarantine. Moreover, AI technology can provide a consistent method for rapid evaluation of high volumes of diagnostic that can reliably exclude images which are negative for findings associated with COVID-19. This decreases the volume of cases passing through to the radiologist without overlooking positive cases. Using AI solutions, progression and regression of positive findings could be monitored more quantitatively and regularly. This could lead to more effective identification and containment of early cases. The study also discovered that a critical existing impediment to effective AI implementation is the lack of COVID-19-related clinical data that can be maintained and processed into easily accessible databases. Integrating COVID-19-related clinical data with existing biobanks, as well as pre-existing patient data, could help bioinformaticians and computational scientists develop a faster and more practical way to useful data-mining.

It is our hypothesis that AI and ML tools can leverage the ability to modify and adapt existing models and combine them with initial clinical understanding to address COVID-19 challenges and the new emerging strains or mutations of the virus. Researchers and scientists are hoping to speed up the development of extremely precise and useful AI, ML, and deep learning technologies to combat COVID-19. If our societies could not reach the best expected AI solutions during this pandemic, we strongly anticipate that AI technology will be of greater help with the next pandemic.

Acknowledgements

The author would like to express his gratitude and grateful appreciation to the Kuwait Foundation for the Advancement of Sciences (KFAS) for financially supporting this project. The project was fully funded by KFAS under project code: PN20-13NH-03.

IntechOpen

IntechOpen

Author details

Naser Zaeri
Faculty of Computer Studies, Arab Open University, Kuwait

*Address all correspondence to: n.zaeri@aou.edu.kw

IntechOpen

© 2021 The Author(s). Licensee IntechOpen. This chapter is distributed under the terms of the Creative Commons Attribution License (http://creativecommons.org/licenses/by/3.0), which permits unrestricted use, distribution, and reproduction in any medium, provided the original work is properly cited. CC BY

References

[1] Sousa, R. T., O. Marques, Iwens I. G. Sene, Anderson S. Soares and L. L. G. D. Oliveira. "Comparative performance analysis of machine learning classifiers and dimensionality reduction algorithms in detection of childhood pneumonia." (2013)

[2] https://www.who.int/emergencies/diseases/novel-coronavirus-2019, 2021

[3] B. Wang, R. Li, Z. Lu, Y. Huang, Does comorbidity increase the risk of patients with COVID-19: evidence from meta-analysis, Aging (Albany NY) 12 (7) (2020) 6049

[4] S. Szymkowski. COVID-19 Shut Down 93% of All US Auto Production. Roadshow, 2020. [Online]. Available: https://www.cnet.com/roadshow/news/covid-19-shut-down-us-autoproductio%n-coronavirus/

[5] Ng et al. Imaging profile of the covid-19 infection: Radiologic findings and literature review. Radiology: Cardiothoracic Imaging, 2(1), 2020

[6] Pham, Q.-V.; Nguyen, D.C.; Huynh-The, T.; Hwang, W.-J.; Pathirana, P.N. Artificial intelligence (AI) and big data for coronavirus (COVID-19) pandemic. 2020, 2020040383

[7] A. Bernheim et al., "Chest CT Findings in Coronavirus Disease-19 (COVID-19): Relationship to Duration of Infection," Radiology, pp. 200463-200463, 2020-Feb-20 2020, doi: 10.1148/radiol.2020200463.

[8] S. Ardabili, *A. Mosavi*, S. S. Band and A. R. Varkonyi-Koczy, "Coronavirus Disease (COVID-19) Global Prediction Using Hybrid Artificial Intelligence Method of ANN Trained with Grey Wolf Optimizer," 2020 IEEE 3rd International Conference and Workshop in Óbuda on Electrical and Power Engineering (CANDO-EPE), Budapest, Hungary, 2020, pp. 000251-000254, doi: 10.1109/CANDO-EPE5 1100.2020.9337757

[9] Tang, L, Tian, C, Meng, Y, Xu, K., "Longitudinal evaluation for COVID-19 chest CT disease progression based on Tchebichef moments," International Journal of Imaging Systems and Technology, pp. 1– 8, 2021, https://doi.org/10.1002/ima.22583

[10] Reza Mohammadi, Iman Shokatian, Mohammad Salehi, Hossein Arabi, Isaac Shiri, Habib Zaidi, "Deep learning-based auto-segmentation of organs at risk in high-dose rate brachytherapy of cervical cancer," Radiotherapy and Oncology, Volume 159, 2021, Pages 231-240, ISSN 0167-8140, https://doi.org/10.1016/j.radonc.2021.03.030

[11] D. -P. Fan et al., "Inf-Net: Automatic COVID-19 Lung Infection Segmentation From CT Images," in IEEE Transactions on Medical Imaging, vol. 39, no. 8, pp. 2626-2637, 2020, doi: 10.1109/TMI.2020.2996645

[12] 7.Y. Feng et al., "COVID-19 with different severities: A multicenter study of clinical features", Amer. J. Respir. Crit. Care Med., vol. 201, no. 11, pp. 1380-1388, 2020

[13] Anand Rao, Global Leader, Artificial Intelligence, PwC and Kay Firth-Butterfield, Head, Artificial Intelligence and Machine Learning, World Economic Forum, "3 ways COVID-19 is transforming advanced analytics and AI," 23 Jul 2020

[14] Zhongxiang Chen, Jun Yang and Binxiang Dai, "Forecast Possible Risk for COVID-19 Epidemic Dissemination under Current Control Strategies in Japan," Int. J. Environ. Res. Public Health 2020, 17, 3872; doi:10.3390/ijerph17113872

[15] EIT-a body of the European Union "Transforming healthcare with AI: The impact on the workforce and organisations,", 2020

[16] Holzinger, A. et al., "What do we need to build explainable AI systems for the medical domain?", arXiv:1712.09923, 2017.

[17] Mohammad (Behdad) Jamshidi et al., "Artificial Intelligence and COVID-19: Deep Learning Approaches for Diagnosis and Treatment," IEEE Special Section On Emerging Deep Learning Theories And Methods For Biomedical Engineering, June 24, 2020

[18] S. Dodge and L. Karam, "Understanding how image quality affects deep neural networks," International Conference on Quality of Multimedia Experience (QoMEX), 2016 http://image-net.org/challenges/LSVRC/2010/results; http://image-net.org/challenges/LSVRC/2017/results.

[19] Daniel Nelson, "Baidu Beats Out Google And Microsoft, Creates New Technique For Language Understanding", Unite. AI, 28 December 2019, https://www.unite.ai/baidu-beats-out-google-and-microsoft-creates-new-technique-for-languageunderstanding/.

[20] "Can science be automated?" ScienceDaily, April 2019, https://www.sciencedaily.com/releases/2019/04/190418105730.htm

[21] Hinton, G., Deep learning—a technology with the potential to transform health care. Jama, 2018, 320(11), pp.1101-1102; Gottesman, O., et al., "Guidelines for reinforcement learning in healthcare". Nature Medicine, 2019, 25(1), pp.16-18

[22] Soroush Nasiriany, Garrett Thomas, William Wang, Alex Yang, Jennifer Listgarten, Anant Sahai, "A Comprehensive Guide to Machine Learning," Department of Electrical Engineering and Computer Sciences University of California, Berkeley, 2019

[23] Garrett Thomas, "Mathematics for Machine Learning" Department of Electrical Engineering and Computer Sciences, University of California, Berkeley, 2018

[24] J. Wan , D. Wang , S.C. Hoi , P. Wu , J. Zhu , Y. Zhang , J Li , Deep learning for con- tent-based image retrieval: a comprehensive study, in: Proceedings of the 22nd ACM international conference on Multimedia, 2014 Nov 3, pp. 157-166

[25] M.A . Wani , F.A . Bhat , S. Afzal , A .I Khan , Advances in Deep Learning, Springer, 2020

[26] Nicolas Coudray, Paolo Santiago Ocampo, Theodore Sakellaropoulos, Navneet Narula, Matija Snuderl, David Fenyo, Andre L Moreira, Narges Razavian, and Aristotelis Tsirigos. Classification and mutation prediction from non–small cell lung cancer histopathology images using deep learning. Nature medicine, 24(10):1559-1567, 2018

[27] Kaiming He, Xiangyu Zhang, Shaoqing Ren, and Jian Sun. Delving deep into rectifiers: Surpassing human-level performance on imagenet classification. In Proceedings of the IEEE international conference on computer vision, pages 1026-1034, 2015

[28] Ng MY, Lee EY, Yang J, et al. Imaging Profile of the COVID-19 Infection: Radiologic Findings and Literature Review. Radiol Cardiothorac Imaging 2020;2(1):e200034

[29] Pan F, Ye T, Sun P, et al. Time Course of Lung Changes On Chest CT During Recovery From 2019 Novel Coronavirus (COVID-19) Pneumonia. Radiology 2020 Feb 13:200370

[30] Chung M, Bernheim A, Mei X, et al. CT Imaging Features of 2019 Novel

Coronavirus (2019-nCoV). Radiology 2020;295(1):202-207.

[31] Song F, Shi N, Shan F, et al. Emerging 2019 Novel Coronavirus (2019-nCoV) Pneumonia. Radiology 2020;295(1):210-217.

[32] Pan Y, Guan H, Zhou S, et al. Initial CT findings and temporal changes in patients with the novel coronavirus pneumonia (2019-nCoV): a study of 63 patients in Wuhan, China. Eur Radiol 2020

[33] Bernheim A, Mei X, Huang M, et al. Chest CT Findings in Coronavirus Disease- 19 (COVID-19): Relationship to Duration of Infection. Radiology 2020 Feb 20:200463

[34] Bai HX, Hsieh B, Xiong Z, et al. Performance of radiologists in differentiating COVID- 19 from viral pneumonia on chest CT. Radiology 2020 Mar 10:200823

[35] Peng, Q.-Y., Wang, X.-T. & Zhang, L.-N. Findings of lung ultrasonography of novel corona virus pneumonia during the 2019-2020 epidemic. Intensive Care Med 1-2 (2020) doi:10.1007/s00134-020-05996-6

[36] Huang, Y. et al. A Preliminary Study on the Ultrasonic Manifestations of Peripulmonary Lesions of Non-Critical Novel Coronavirus Pneumonia (COVID-19). https://papers.ssrn.com/abstract=3544750 (2020) doi:10.2139/ssrn.3544750

[37] Bertalmio, M., Bertozzi, A. L. & Sapiro, G. Navier-stokes, fluid dynamics, and image and video inpainting. in Proceedings of the 2001 IEEE Computer Society Conference on Computer Vision and Pattern Recognition. CVPR 2001 vol. 1, 2001

[38] Buda, N., Segura-Grau, E., Cylwik, J. & Wełnicki, M. Lung ultrasound in the diagnosis of COVID-19 infection - A case series and review of the literature. Advances in Medical Sciences 65, 378-385 (2020)

[39] Brahier, T. et al. Lung ultrasonography for risk stratification in patients with COVID-19: a prospective observational cohort study. Clinical Infectious Diseases (2020) doi:10.1093/cid/ciaa1408

[40] Karagöz, A., Saglam, C., Demirbas, H. B., Korkut, S. & Ünlüer, E. E. Accuracy of Bedside Lung Ultrasound as a Rapid Triage Tool for Suspected Covid-19 Cases. Ultrasound Quarterly 36, 339-344 (2020)

[41] H. Zhang , G. Chen , X. Li , Resource management in cloud computing with optimal pricing policies, Comput. Syst. Sci. Eng. 34 (4) (2019) 249-254

[42] M.J. Van Der Donckt , D. Weyns , M.U. Iftikhar , R.K. Singh , Cost-benefit analysis at runtime for self-adaptive systems applied to an internet of things application., in: Proceedings of the ENASE, 2018, pp. 478-490

[43] D. Gupta , O. Kayode , S. Bhatt , M. Gupta , A.S. Tosun , Learner's Dilemma: IoT devices training strategies in collaborative deep learning, IEEE 6th World Forum Internet Things (WF-IoT) (2020)

[44] Bassetti, M., Kollef, M. H. & Timsit, J. F. Bacterial and fungal superinfections in critically ill patients with COVID-19. Intensive Care Med. 46, 2071-2074 (2020)

[45] Lin Li,1b, Lixin Qin, Zeguo Xu, Youbing Yin, Xin Wang, Bin Kong, Junjie Bai, Yi Lu, Zhenghan Fang, Qi Song, Kunlin Cao, Daliang Liu, Guisheng Wang, Qizhong Xu, Xisheng Fang, Shiqin Zhang, Juan Xia, Jun Xia, "Artificial Intelligence Distinguishes COVID-19 from Community Acquired Pneumonia on Chest CT", Radiology

[46] Chuangsheng Zheng, Xianbo Deng, Qiang Fu1, Qiang Zhou, Jiapei Feng, Hui Ma, Wenyu Liu, Xinggang Wang, "Deep Learning-based Detection for COVID-19 from Chest CT using Weak Label," medRxiv 2020.03.12.20027185; doi: https://doi.org/10.1101/2020.03.12.20027185

[47] O. Gozes, M. Frid-Adar, H. Greenspan, P. D. Browning, H. Zhang, W. Ji, et al., "Rapid AI development cycle for the coronavirus (covid-19) pandemic: Initial results for automated detection & patient monitoring using deep learning ct image analysis," arXiv:2003.05037, 2020

[48] Barstugan, M., Ozkaya, U., and Ozturk, S., "Coronavirus (COVID-19) Classification using CT Images by Machine Learning Methods", arXiv e-prints, 2020

[49] Damiano Caruso, Marta Zerunian, Michela Polici, Francesco Pucciarelli, Tiziano Polidori, Carlotta Rucci, Gisella Guido, Benedetta Bracci, Chiara De Dominicis, Andrea Laghi, "Chest CT Features of COVID-19 in Rome, Italy," Radiology: Volume 296: Number 2—August 2020

[50] Salehi S, Abedi A, Balakrishnan S, Gholamrezanezhad A. Coronavirus Disease 2019 (COVID-19): A Systematic Review of Imaging Findings in 919 Patients. AJR Am J Roentgenol 2020 Mar 14:1-7

[51] Chung M, Bernheim A, Mei X, et al. CT Imaging Features of 2019 Novel Coronavirus (2019-nCoV). Radiology 2020;295(1):202-207.

[52] Xiaowei Xu, Xiangao Jiang, Chunlian Mac, Peng Dud, Xukun Li, Shuangzhi Lv, Liang Yu, Qin Ni, Yanfei Chen, Junwei Su, Guanjing Lang, Yongtao Li, Hong Zhao, Jun Liu, Kaijin Xu , Lingxiang Ruan, Jifang Sheng, Yunqing Qiu, Wei Wua, Tingbo Liang, Lanjuan Li, "A Deep Learning System to Screen Novel Coronavirus Disease 2019 Pneumonia," Engineering, 2020

[53] Maria Paola Belfiore, Fabrizio Urraro, Roberta Grassi, Giuliana Giacobbe, Gianluigi Patelli, Salvatore Cappabianca, Alfonso Reginelli, "Artificial intelligence to codify lung CT in Covid-19 patients," La radiologia medica (2020) 125:500-504, https://doi.org/10.1007/s11547-020-01195-x

[54] Xueyan Mei et al., "Artificial intelligence–enabled rapid diagnosis of patients with COVID-19," Nature Medicine, VOL 26, August 2020, pp. 1224-1228, www.nature.com/naturemedicine

[55] Kuruvilla, J., Gunavathi, K.: Lung cancer classification using neural networks for ct images. Computer methods and programs in biomedicine 113(1), 202-209 (2014)

[56] Brunese, L., Mercaldo, F., Reginelli, A. & Santone, A. Explainable Deep Learning for Pulmonary Disease and Coronavirus COVID-19 Detection from X-rays. Computer Methods and Programs in Biomedicine 196, 105608 (2020)

[57] Wikramaratna, P. S., Paton, R. S., Ghafari, M. & Lourenço, J. Estimating the false-negative test probability of SARS-CoV-2 by RT-PCR. medRxiv 2020.04.05.20053355 (2020) doi:10.1101/2020.04.05.20053355

[58] Born, J. et al. POCOVID-Net: Automatic Detection of COVID-19 From a New Lung Ultrasound Imaging Dataset (POCUS). arXiv:2004.12084 [cs, eess] (2020)

[59] Harrison X. Bai, Robin Wang, Zeng Xiong, Ben Hsieh, Ken Chang, Kasey Halsey, Thi My Linh Tran, Ji Whae Choi, Dong-Cui Wang, Lin-Bo Shi, Ji Mei, Xiao-Long Jiang, Ian Pan, Qiu-Hua Zeng, Ping-Feng Hu, Yi-Hui Li, Fei-Xian Fu, Raymond Y. Huang, Ronnie Sebro,

Qi-Zhi Yu, Michael K. Atalay, Wei-Hua Liao, "Artificial Intelligence Augmentation of Radiologist Performance in Distinguishing COVID-19 from Pneumonia of Other Origin at Chest CT," Radiology 2020; 296:E156–E165, https://doi.org/10.1148/radiol.2020201491, Volume 296: Number 3—September 2020

[60] Rajesh Kumar, Abdullah Aman Khan, Sinmin Zhang, WenYong Wang, Yousif Abuidris, Waqas Amin , and Jay Kumar, "Blockchain-Federated-Learning and Deep Learning Models for COVID-19 detection using CT Imaging," JOURNAL OF LATEX CLASS FILES, VOL. 14, NO. 8, AUGUST 2020

[61] Bourcier, J.-E. et al. Performance comparison of lung ultrasound and chest x-ray for the diagnosis of pneumonia in the ED. The American Journal of Emergency Medicine 32, 115-118 (2014)

[62] Hoon Ko, Heewon Chung, Wu Seong Kang, Kyung Won Kim, Youngbin Shin, Seung Ji Kang, Jae Hoon Lee, Young Jun Kim, Nan Yeol Kim, Hyunseok Jung, Jinseok Lee, "COVID-19 Pneumonia Diagnosis Using a Simple 2D Deep Learning Framework With a Single Chest CT Image: Model Development and Validation," JOURNAL OF MEDICAL INTERNET RESEARCH, 2020, vol. 22, iss. 6, e19569

[63] S. Ardabili, *A. Mosavi*, S. S. Band and A. R. Varkonyi-Koczy, "Coronavirus Disease (COVID-19) Global Prediction Using Hybrid Artificial Intelligence Method of ANN Trained with Grey Wolf Optimizer," 2020 IEEE 3rd International Conference and Workshop in Óbuda on Electrical and Power Engineering (CANDO-EPE), Budapest, Hungary, 2020, pp. 000251-000254, doi: 10.1109/CANDO-EPE51100.2020.9337757

[64] F. Gao, K. Deng and C. Hu, "Construction of TCM Health Management Model for Patients with Convalescence of Coronavirus Disease Based on Artificial Intelligence," 2020 International Conference on Big Data and Informatization Education (ICBDIE), Zhangjiajie, China, 2020, pp. 417-420, doi: 10.1109/ICBDIE50010.2020.00104

[65] S. Tabik et al., "COVIDGR Dataset and COVID-SDNet Methodology for Predicting COVID-19 Based on Chest X-Ray Images," in IEEE Journal of Biomedical and Health Informatics, vol. 24, no. 12, pp. 3595-3605, Dec. 2020, doi: 10.1109/JBHI.2020.3037127

[66] D. -P. Fan et al., "Inf-Net: Automatic COVID-19 Lung Infection Segmentation From CT Images," in IEEE Transactions on Medical Imaging, vol. 39, no. 8, pp. 2626-2637, Aug. 2020, doi: 10.1109/TMI.2020.2996645

[67] F. Shi et al., "Review of Artificial Intelligence Techniques in Imaging Data Acquisition, Segmentation, and Diagnosis for COVID-19," in IEEE Reviews in Biomedical Engineering, vol. 14, pp. 4-15, 2021, doi: 10.1109/RBME.2020.2987975

[68] Di Dong, Zhenchao Tang, Shuo Wang, Hui Hui, Lixin Gong, Yao Lu, Zhong Xue, Hongen liao, Fang Chen, Fan Yang, Ronghua Jin, Kun Wang, Zhenyu Liu, Jingwei Wei, Wei Mu, Hui Zhang, Jingying Jiang, Jie Tian, Hongjun Li, "The role of imaging in the detection and management of COVID-19: a review," IEEE DOI 10.1109/RBME.2020.2990959

[69] Beovic, B. et al. Antibiotic use in patients with COVID-19: A 'snapshot' Infectious Diseases International Research Initiative (ID-IRI) survey. J. Antimicrob. Chemother. 75, 3386-3390 (2020)

[70] Tabassum, N., Zhang, H. & Stebbing, J. Repurposing Fostamatinib to combat SARS-CoV-2-induced acute

lung injury. Cell Reports Med. 1, 100145 (2020)

[71] Shuo Jin et al., "AI-assisted CT imaging analysis for COVID-19 screening: Building and deploying a medical AI system in four weeks," medRxiv preprint doi: https://doi.org/10.1101/2020.03.19.20039354

[72] Cheng Jin, Weixiang Chen, Yukun Cao, Zhanwei Xu, Zimeng Tan, Xin Zhang, Lei Deng, Chuansheng Zheng, Jie Zhou, Heshui Shi, Jianjiang Feng, "Development and evaluation of an artificial intelligence system for COVID-19 diagnosis,", NATURE COMMUNICATIONS, (2020) 11:5088, https://doi.org/10.1038/s41467-020-18685-1, www.nature.com/naturecommunications

[73] Jin et al., "A rapid advice guideline for the diagnosis and treatment of 2019 novel coronavirus (2019-nCoV) infected pneumonia (standard version),"Military Medical Research (2020) 7:4 https://doi.org/10.1186/s40779-020-0233-6

[74] Jun Chen et al. "Deep learning-based model for detecting 2019 novel coronavirus pneumonia on high-resolution computed tomography: a prospective study," medRxiv preprint doi: https://doi.org/10.1101/2020.02.25.20021568

[75] Chen J, Wu L, Zhang J, Zhang L, Gong D, Zhao Y, Chen Q, Huang S, Yang M, Yang X, Hu S, Wang Y, Hu X, Zheng B, Zhang K, Wu H, Dong Z, Xu Y, Zhu Y, Chen X, Zhang M, Yu L, Cheng F, Yu H, Open-access website available at: http://121.40.75.149/znyx-ncov/index

[76] Dasari Naga Vinod, S.R.S. Prabaharan, "Data science and the role of Artificial Intelligence in achieving the fast diagnosis of Covid-19," Chaos, Solitons and Fractals 140 (2020) 110182

[77] Christopher Gieraerts, Anthony Dangis, Lode Janssen, Annick Demeyere, Yves De Bruecker, Nele De Brucker, Annelies van Den Bergh, Tine Lauwerier, André Heremans, Eric Frans, Michaël Laurent, Bavo Ector, John Roosen, Annick Smismans, Johan Frans, Marc Gillis, Rolf Symons, "Prognostic Value and Reproducibility of AI-assisted Analysis of Lung Involvement in COVID-19 on Low-Dose Submillisievert Chest CT: Sample Size Implications for Clinical Trials," Radiology: Cardiothoracic Imaging, 2020

[78] Wu J, Feng CL, Xian XY, Qiang J, et al (2020) Novel Coronavirus Pneumonia (COVID-19) CT Distribution and Sign Features. Zhonghua Jie He He Hu Xi Za ZhiPMID: 32125131 DOI: 10.3760 / cma.j.cn112147-20200217-00106

[79] Bernheim A, Mei X, Huang M, et al (2020) Chest CT Findings in Coronavirus Disease-19 (CO-VID-19): Relationship to Duration of Infection. Radiology https://doi.org/10.1148/radiol. 2020200463

[80] S. Ying, S. Zheng, L. Li, X. Zhang, X. Zhang, Z. Huang, et al., "Deep learning enables accurate diagnosis of novel Coronavirus (COVID-19) with CT images.," MedRxiv, 2020

[81] ShuaiWang, Bo Kang, Jinlu Ma, Xianjun Zeng, Mingming Xiao, Jia Guo, Mengjiao Cai, Jingyi Yang, Yaodong Li, Xiangfei Meng, et al. 2020. Adeep learning algorithm using CT images to screen for Corona Virus Disease (COVID-19). MedRxiv (2020).

[82] Manjurul Ahsan, Kishor Datta Gupta, Mohammad Maminur Islam, Sajib Sen, Lutfar Rahman, Mohammad Shakhawat Hossain, "Study of Different Deep Learning Approach With Explainable AI For Screening Patients With Covid-19 Symptoms: Using Ct Scan and Chest X-Ray Image Dataset," arXiv:2007.12525v1 [eess.IV] 24 Jul 2020

[83] Mucahid Barstugan, Umut Ozkaya, and Saban Ozturk. 2020. Coronavirus (covid-19) classification using ct images by machine learning methods. arXiv preprint arXiv:2003.09424 (2020).

[84] Rassa Ghavami Modegh et al., "Accurate and Rapid Diagnosis of COVID-19 Pneumonia with Batch Effect Removal of Chest CT-Scans and Interpretable Artificial Intelligence," arXiv:2011.11736v2, 2021

[85] Dan Nguyen, Fernando Kay, Jun Tan, Yulong Yan, Yee Seng Ng, Puneeth Iyengar, Ron Peshock, Steve Jiang, "Deep learning–based COVID-19 pneumonia classification using chest CT images: model generalizability," 2021

[86] Vruddhi Shah, Rinkal Keniya, Akanksha Shridharani, Manav Punjabi, Jainam Shah, Ninad Mehendale, "Diagnosis of COVID-19 using CT scan images and deep learning techniques," Emergency Radiology, https://doi.org/10.1007/s10140-020-01886-y, 2021

[87] Fei Shan, Yaozong Gao, Jun Wang, Weiya Shi, Nannan Shi, Miaofei Han, Zhong Xue, Dinggang Shen, Yuxin Shi, "Abnormal lung quantification in chest CT images of COVID-19 patients with deep learning and its application to severity prediction," International Journal of Medical Physics Research and Practice, 2020, https://doi.org/10.1002/mp.14609

[88] C. Zheng, X. Deng, Q. Fu, Q. Zhou, J. Feng, H. Ma, et al., "Deep learning-based detection for COVID-19 from chest CT using weak label," MedRxiv, 2020

[89] L. Huang, R. Han, T. Ai, P. Yu, H. Kang, Q. Tao, et al., "Serial quantitative chest CT assessment of COVID-19: Deep-Learning Approach," Radiology: Cardiothoracic Imaging, vol. 2, p. e200075, 2020

[90] Lionel Roques, Etienne Klein, Julien Papa, Antoine Sar and Samuel Soubeyrand, "Using early data to estimate the actual infection fatality ratio from COVID-19 in France ," Biology doi: 10.3390/biology9050097

[91] Athanasios S. Fokas, Nikolaos Dikaios, George A. Kastis, "COVID-19: Predictive Mathematical Models for the Number of Deaths in South Korea, Italy, Spain, France, UK, Germany, and USA," doi: https://doi.org/10.1101/2020.05.08.20095489

[92] I. Apostolopoulos, S. Aznaouridis, and M. Tzani. Extracting possibly representative covid-19 biomarkers from x-ray images with deep learning approach and image data related to pulmonary diseases. arXiv preprint arXiv:2004.00338, 2020

[93] Song, P., Wang, L., Zhou, Y., He, J., Zhu, B., Wang, F., Tang, L., and Eisenberg, M. (2020). An Epidemiological Forecast Model and Software Assessing Interventions on COVID-19 Epidemic in China. medRxiv, (https://doi.org/10.1101/2020.02.29.20029421)

[94] Zhou, Z., Siddiquee, M. M. R., Tajbakhsh, N. & Liang, J. UNet++: A nested U-Net architecture for medical image segmentation. In Deep Learning in Medical Image Analysis and Multimodal Learning for Clinical Decision Support, 3-11 (Springer, 2018).

[95] Long, J., Shelhamer, E. & Darrell, T. Fully convolutional networks for semantic segmentation. In Proceedings of the IEEE Conference on Computer Vision and Pattern Recognition, 3431-3440 (2015).

[96] Tang Z, Zhao W, Xie X, Zhong Z, Shi F, Liu J, et al. Severity assessment of coronavirus disease 2019 (COVID-19) using quantitative features from chest CT images. arXiv. (2020) 2003.11988. Available online at: https://arxiv.org/ abs/2003.11988 (accessed May 10, 2020)

[97] Y. Jiang, H. Chen, M. Loew and H. Ko, "COVID-19 CT Image Synthesis With a Conditional Generative Adversarial Network," in IEEE Journal of Biomedical and Health Informatics, vol. 25, no. 2, pp. 441-452, Feb. 2021, doi: 10.1109/JBHI.2020.3042523

[98] Khalid El Asnaoui, Youness Chawki, and Ali Idri. 2020. Automated methods for detection and classification pneumonia based on x-ray images using deep learning. arXiv preprint arXiv:2003.14363 (2020)

[99] Li K, Wu J, Wu F, Guo D, Chen L, Fang Z, Li C. The Clinical and Chest CT Features Associated With Severe and Critical COVID-19 Pneumonia. Invest Radiol 2020;55(6):327-331. doi: 10.1097/RLI.0000000000000672

[100] Jocelyn Zhu, Beiyi Shen, Almas Abbasi, Mahsa Hoshmand-Kochi, Haifang Li, Tim Q. Duong, "Deep transfer learning artificial intelligence accurately stages COVID-19 lung disease severity on portable chest radiographs," PLOS ONE, https://doi.org/10.1371/journal.pone.0236621, 2020

[101] Jasjit S. Suri et al., "COVID-19 pathways for brain and heart injury in comorbidity patients: A role of medical imaging and artificial intelligence-based COVID severity classification: A review," Computers in Biology and Medicine 124 (2020) 103960